THE LOCALIZATION AND DYNAMICS OF ACTIN IN

ASPERGILLUS NIDULANS

An Undergraduate Research Scholars Thesis

by

ANGELYN E HILTON

Submitted to Honors and Undergraduate Research
Texas A&M University
in partial fulfillment of the requirements for the designation as

UNDERGRADUATE RESEARCH SCHOLAR

Approved by
Research Advisor: Dr. Brian Shaw

May 2013

Major: Bioenvironmental Sciences
Department: Plant Pathology and Microbiology

TABLE OF CONTENTS

Page

ABSTRACT

The Localization and Dynamics of Actin in *Aspergillus nidulans* (May 2013).

Angelyn E. Hilton
Department of
Plant Pathology and Microbiology
Texas A&M University

Research Advisor: Dr. Brian Shaw
Department of
Plant Pathology and Microbiology

F-actin, a cytoskeletal component of microfilaments, plays an important role in fungal growth and development. It can be found in different forms, including cables and patches. Lifeact is a fluorescent reporter of actin dynamics in live cells. The Lifeact construct was transformed into *Aspergillus nidulans* to monitor the dynamics of actin using time-lapse imaging and fluorescence microscopy. Subapical collars, composed of F-actin patches associated with endocytosis, have been found to be necessary components for polar growth in the hyphae of *A. nidulans*. Actin cables, which form the contractile actin ring (CAR), were observed during the formation of the septum. Actin rings were also localized to sites where new branches were formed. Actin cables, coalescing to form the apical actin array (AAA), localized to sites of new branch formation. The AAA also localized to the site where polarity was established in conidial germination. As germ tube development was initiated, the AAA simultaneously migrated into the site of new growth. The AAA has been documented in the tips of other growing fungi. Similar patterns were noted in *A. nidulans.* Actin dynamics were documented during conidial and hyphal anastomosis. Actin cables localized to site of fusion in each cell. In addition, subapical actin webs (SAWs), or

masses of F-actin cables, were found distal to the apex in other hyphae. Future research is needed to understand the mechanisms of the SAW structure. Through the understanding of actin dynamics in the developmental stages of filamentous fungi, we may be able to develop ways to control fungal diseases of plants and animals.

ACKNOWLEDGEMENTS

I would like to thank Nick Read, Alexander Lichius and Adokiye Berepiki for providing the Lifeact construct. Also, I would like to thank graduate student, Laura Quintanilla, of the Department of Plant Pathology and Microbiology at Texas A&M University for all of her help, generosity and support in the laboratory. In addition, I could not have written this thesis or performed my research without the assistance from my research advisor, Dr. Brian Shaw, Associate Professor of the Department of Plant Pathology and Microbiology.

NOMENCLATURE

Arp2/3	Actin-related protein 2/3
GTPases	Guanine Nucleotide Triphosphatases
FH	Formin Homology domain
GFP	Green Fluorescent Protein
RFP	Red Fluorescent Protein
CAR	Contractile Actin Ring
CAT	Conidial Anastomosis Tube
AAA	Apical Actin Array
SAW	Subapical Actin Web

CHAPTER I

INTRODUCTION

The filamentous fungal cell, or tubular hyphae, is morphologically maintained by a complex cytoskeleton. Like all eukaryotes the cytoskeleton plays an important role in cellular support, as well as growth and development. This skeletal structure has also been indicated in the regulation of different transport mechanisms, including endocytosis and exocytosis. Fitness of the fungus is highly dependent on cytoskeletal stability. The cytoskeleton must behave effectively for the fungus to uptake nutrients, and to sustain the functional properties of higher order structures within the cell (Lichius, et. al, 2011). Through the research and understanding of the fungal cytoskeleton, a broader approach to addressing plant and human mycoses can be developed.

Actin protein of the fungal cytoskeleton

The fungal cytoskeleton is composed of three polymer structures, actin microfilaments, microtubules and septins. Actin microfilaments, in particular, have recently attracted the research of many fungal biologists to discover how the protein dynamics support fungal growth and development. The aim of this study is to document actin localization and dynamics inside the fungal cell of *Aspergillus nidulans. A. nidulans* is a saprotrophic, model organism that has been used in many experiments and whose traits are genetically conserved amongst other filamentous fungi, such as *Neurospora crassa*. *A. nidulans* is closely related to *A. niger, A. fumigatus* and *A. flavus*, three fungi which are important in industry, medicine and agriculture, respectively. Furthermore, with limited resources available to confront fungi-related epidemics, *A. nidulans* can be used to find viable treatments for certain fungal diseases.

Actin is a highly conserved, protein that can be found in the majority of higher eukaryotes (Berepiki, et al., 2011). The human muscular complex contains actin, which is vital to our own physical maturation, movement, and respiratory function. Continued research on the study of actin can provide insight into eukaryote morphology and diseases associated with abnormalities in the expression of actin, such as muscular dystrophy and Alzheimers (Norwood, et al, 2000; Penzes, et al., 2011). Actin is composed of monomeric gobular actin, or G-actin, which undergoes polymerization to form filamentous F-actin. The F-actin will then aggregate to form patches, cables, and rings (Lichius, et al., 2011).

F-actin polymerization is nucleated by a complex of proteins called formins, or actin-related protein (Arp2/3), which are homologous throughout a wide range of multicellular organisms, including animals, fungi, plants and protists (Goode and Eck, 2007). Formin proteins are not only required for the regulation of actin filaments, but also in a number of different cellular processes such as the development of the microtubule cytoskeleton. The formin proteins which generate actin filaments are activated by the members of the Rho family, signaling proteins composed of small guanine nucleotide triphosphatases (GTPases) (Seifert, 2008). This family of proteins is conserved in all eukaryotes and has been the subject for extensive research amongst a variety of organisms. Some fungal species encode multiple distinct formins, such as *S. cerevisiae* which encodes for two or *Schizosaccharomyces pombe* which encodes three. *A. nidulans* and *N. crassa* each encode for one distinct formin; *A. nidulan*'s formin is known as *sepA* (Xiang and Plamann, 2003; Harris, 2001).

Actin undergoes treadmilling, in which the barbed, plus end elongates through the fast insertion of actin subunits, and its 'pointed,' minus end contracts due to a slower rate of polymerization (Lichius, et al., 2011). When Rho GTPases signal the site-specific formin proteins, the formin homology (FH) domain, initiate F-actin assembly by quickly nucleating unbranched actin subunits at the barbed end of the growing filament (Goode and Eck, 2007). Once fully assembled, the FH can give rise to the formation of higher order F-actin structures, such as patches and cables.

There are several live cell markers that have been created to observe actin structural dynamics inside the growing fungal cell. Prior to the development of these live cell markers, researchers were only able to observe the morphology of the fixed/dead cells in filamentous fungi and other microorganisms. This demonstrates the importance of documenting the physiological processes and dynamics inside the live cells of model organisms. One particular live cell marker, LifeAct, is a construct which consists of a 17 aa peptide developed from the actin binding 140 protein (Abp140) of *S. cerevisiae* (Lichius, et al., 2011; Delgado, et al, 2011; Riedl, et al., 2008). Abp140 binds to the actin and is then fused to a green or red fluorescent protein (GFP or TagRFP, respectively). This allows for the tracking of actin localization through fluorescent microscopy. In addition, the Lifeact cassette can be combined with a promoter which is regulated to control actin expression. When tested on several types of eukaryotic cells, including both fungal and mammalian cells, LifeAct-GFP and -TagRFP were shown to be reliable markers for both G- and F-actin assemblages and have no damaging effects on cellular processes (Riedl, et al., 2008). Therefore, accurate documentation of actin dynamics can be obtained in order to understand the different roles of F-actin within the fungal cell. Strains of *A. nidulans* expressing

LifeAct-GFP or -TagRFP were constructed by graduate student, Ms. Laura Quintanilla in the molecular fungal biology laboratory of Dr. Brian Shaw at Texas A&M University. The Lifeact cassette combined with the regulatory promoter, *Ccg-1*, was donated by Nick Read, Alexander Lichius and Adokiye Berepiki. Ms. Laura Quintanilla is responsible for the construction of the Lifeact cassette combined with the regulatory promoter, *niiA.*

Developmental stages of filamentous fungi

Through the use of LifeAct, researchers have been able to identify several different molecular processes with which actin is associated throughout the life cycles of filamentous fungi. Perhaps the most rudimentary of the developmental stages is hyphal growth. Hyphae grow exclusively by apical growth, meaning that new growth occurs at the tip. The Spitzenkörper, an organelle located within the apex of the hyphae, is associated with this polarized growth. Studies using LifeAct have shown that F-actin patches will congregate around the Spitzenkörper and in the area of new growth, indicating that F-actin may also be required in cellular development. This assemblage of actin patches is referred to as a subapical, endocytic collar and has been observed in both *N. crassa* and *A. nidulans* (Berepiki, et al., 2010; Shaw, et al., 2011; Delgado, et al., 2011). When treated with an F-actin inhibitor, the subapical collar dissipates and cellular elongation is diminished, providing evidence that actin is necessary for the growth of the hyphae (Berepiki, et al., 2010).

Septation

Contractile actin rings (CARs) have been documented to localize at new sites of septation in *N. crassa* and *A. nidulans* (Berepiki, et al., 2010; Harris, 2001). Septation in filamentous fungi

occurs during both vegetative growth and conidiation, and results in the formation of a chitin-based cross wall known as a septum (Momany and Hamer, 1997). Septation in filamentous fungi is comparative to cytokinesis occurring in animal cells and serves as a semipermeable band which differentiates fungal cells within a hyphae. Septation is important in the regulation of cellular transport mechanisms of both nutrients and other structures, such as nuclei. *A. nidulans* will undergo two or three rounds of mitosis, so that the apical cell contains eight nuclei, prior to the assembly of the septum. It is theorized that the synthesis of the CAR is site-specific and triggered by mitotic divisions which signal for septation to occur (Harris, 2001). When the *SepA* formin is inhibited in *A. nidulans*, mutants become sensitive to temperature, display wide hyphae with delayed septation, and experience abnormal conidiation. This indicates that the CAR is essential to the development of septa and fungal fitness, which is significantly decreased in the absence of the formin.

Branch formation

Actin is seen in other areas of new growth as well, such as branch formation. Branching allows the fungus to colonize a nutrient substrate by occupying a greater surface area in the formation of the mycelium. Branching patterns in filamentous fungi include both apical and lateral branching and have been documented in *A. nidulans, A. niger,* and *N. crassa* (Harris, 2008). Apical branching generally occurs when an abnormality of exocytic vesicles arises and leads to the development of a secondary hyphal tip, also known as tip splitting. Lateral branching is considered to be a normal pattern of growth and generally develops distal to the hyphal tip. Actin cables and patches will aggregate to form actin arrays around areas of lateral and apical

branch formation and appear to fill an important niche in establishing the network of the mycelial thallus (Berepiki, et al., 2011).

Conidial germination

Similar to other filamentous fungi, *A. nidulans* reproduces by means of asexual spores, or conidia. Conidial development begins with the formation of a specialized, asexual fruiting body referred to as the condiophore (Krijgsheld, et al., 2012). When released from the conidiophore, non-motile conidia are dispersed by wind or rain. In appropriate environmental conditions, including the presence of glucose and water, these conidia will germinate, leading to hyphal morphogenesis. Hyphae apically elongate and eventually differentiate into sub-apical, cellular compartments via septation (Takeshita and Fischer, 2011). Once septation has occurred, hyphae form lateral branches allowing for the establishment of the complex mycelia. Therefore, conidia are a basic component for the initiation of the lifecycle of the fungus. Asexual conidiospores are not only important in the propagation of the fungus, but can also serve as "genomic safe houses" in adverse environmental conditions (Osherov and May, 2001). In *A. nidulans*, conidia can be stored for extended periods of time without degradation to the cell or traceable metabolic activity.

Cytoskeletal components, such as actin, are necessary for the establishment and maintenance of polarity in germinating conidia (Momany, 2002; Takeshita and Fischer, 2011). However, it is still largely unknown how actin cables and patches will localize inside the conidia during hyphal morphogenesis. Cell end markers, such as TeaA and TeaC, interact with the SepA formin to trigger the production of F-actin inside the cell. The conidium swells, establishing polarity to

site where germ tube formation will occur. Once the primary germ tube has formed, septation must be initiated before a secondary germ tube will appear. The formation of the secondary germination site most often occurs approximately antipole to the site of the primary germ tube. It is hypothesized that actin cables and patches will exhibit similar patterns inside the condium as has been observed in the establishment of polarity during other stages of development, such as hyphal tip growth and branch formation.

Conidial and hyphal anastomosis

Conidial and hyphal fusion or anastomosis can occur in *A. nidulans,* however, the phenomena has not been as extensively studied as in other filamentous fungi, such as *N. crassa.* Anastomosis occurs when cells in close proximity establish connection through the formation of a fusion bridge between conidia, a conidium and germ tube, or between two hyphae (Krijgsheld, et al., 2012). Cell fusion can serve as a means for cells to exchange nutrients or genetic material. This fusion may occur within or between *Aspergillus* strains or species, and has even been documented to occur between the two species, *Aspergillus* and *Penecillium* (Ishitani and Sakaguchi, 1956). However anastomosis between strains or species of filamentous fungi, including *A. nidulans,* can lead to heterokaryon incompatibility (Anwar, et al., 1993; Ishikawa, et al., 2012; Krijgsheld, et al., 2012; Glass, et al. 2000). Evidence shows that *A. nidulans* possess at least eight heterokaryon (*het*) loci which, when regulated by an allelic system, may result in vegetative incompatibility (Glass, et al., 2000).

Conidial anastomosis tubes (CATs) have been documented in 73 species and 21 genera of filamentous fungi, including *A. nidulans* (Roca, et al., 2005). In *Colletotrichum lindemuthianum* and *N. crassa,* CATs are morphologically distinct and under different genetic regulation than that of germ tubes. Unlike germ tubes, CATs are thin tubular cell structures which converge towards one another from coinciding conidiospores. It is theorized that CATs will form in order to increase fitness by improving the establishment of the mycelia in nutrient deficient media. In addition, horizontal gene transfer may facilitate diversity amongst asexual fungi or in species where sexual reproduction is uncommon. Actin dynamics have been studied during CAT formation in *N. crassa* but are yet to be documented in *A. nidulans* (Read, et al., 2012). Filamentous actin, but not microtubules, was found to be required for CAT morphogenesis. This is contrary to the cytoskeletal requirements for the establishment and maintenance of polarity in hyphal growth and germ tube development.

Hyphal anastomosis occurs when two hyphae form a fusion bridge, establishing a connection between their cellular compartments. Like that of CAT formation, hyphal fusion is recognized in *A. nidulans.* However it has not been as extensively reported in the literature in comparison to other filamentous fungal species, such as *N. crassa.* Many researchers speculate that hyphal anastomosis increases interconnectedness throughout the mycelium by intracellular communication, improving colony maintenance, and by allowing for the transfer of nutrients and water between cells (Hickey, et al., 2002; Shinn-Thomas & Mohler, 2011). Fusion bridges are morphologically and physiologically distinct from conidial germ tubes, mature hyphae and lateral branches (Glass, et al., 2004). Hyphae initiate fusion bridges which grow in a polar direction towards one another. Once the fusion bridges meet, polarized development ceases and

isotropic growth proceeds. The cells eventually fuse, breaking down cell walls, and allowing for the free flow of nutrients and cellular components, such as cytoplasm and nuclei. Cell-to-cell connections are also more common in the interior of the colony, where mature hyphae are present, as opposed to the periphery of the mycelia in which new growth is occurring (Hickey, et al., 2002; Kasuga, et al., 2008). Actin dynamics during hyphal anastomosis still remains unexplored in filamentous fungi. Although, evidence has been provided that the development of anastomosis tubes between hyphae is mediated by actin related genes conserved in *S. cerevisiae* and *N. crassa* (Glass, et al., 2004).

Actin arrays

Apical actin arrays (AAAs) are the dense patchworks of actin cables and rings that have been observed in the apex of the filamentous fungal species, *N. crassa* and *A. nidulans* (Lichius, et al., 2011; Quintanilla, 2013). The AAA appears prior to and during conidial germination and lateral branch formation (Lichius, et al., 2011). Subapical actin webs (SAWs) have also been documented in *A. nidulans,* although the mechanism of the SAW structure is still largely unknown. The SAW, similar to the AAA, is composed of actin cables that coalesce to form a mesh-like structure. My hypothesis is that SAWs will form around areas of new growth and may affect the growth rates of growing hyphae within the mycelium.

In conclusion, further monitoring and documentation of actin structures in *A. nidulans* is needed to make a determination of the exact functions of actin filaments throughout the life cycle of the fungus. The purpose of this experiment is to achieve an understanding of the dynamics of actin within the fungal cell. The images generated will provide evidence into the functions of actin in

A. nidulans. It is expected that there will be new information gathered on how actin is involved in hyphal development, particularly regarding the extensive meshwork of actin found just behind the advancing apex of growing cells. There is also the possibility that differences can be identified when comparing the data from other species.

CHAPTER II

METHODS

The Lifeact construct

The Lifeact construct, which is under the promoter *Ccg-1*, is light regulated and was a gift of Adokiye Beripiki, Alexander Lichius and Nick D. Read. Another *A. nidulans* expression vector was created by Ms. Laura Quintanilla by combining the nitrate/ammonia regulatable *niiA* promoter with the Lifeact:RFP cassette using standard fusion PCR protocols (Table 1)(Berepiki et al, 2010; Hervas-Aguilar and Penalva, 2010; Quintanilla, 2013).

Fitness tests

The relative fitness of the wildtype strain A773 was compared to the Lifeact-GFP strain, G-11, and the wildtype strain LQ-1 to the Lifeact-RFP strain, rss3, was measured. Production of conidia and growth rate of mycelia were recorded in this study.

Conidia production

Conidia were collected from 7-day old cultures by scraping plates using a glass pipette and washing with 2 ml of sterile H_2O. The solution was diluted to a 0.1x concentration before counting conidia using a hemocytometer and a basic compound microscope. The number of spores per cm^2 was then calculated using the formula, (#spores*concentration*10). For each strain, n=6. A two-tailed student's T-test assuming unequal variances was then performed to determine if there was a significant difference in the conidia production per µL between the wildtype and the Lifeact expressing GFP and RFP strains ($p<.05$).

Growth rate of mycelia

A 10 μL solution, containing 10^6 spores, was spot inoculated onto four types of fully supplemented minimal media containing different concentrations of sodium nitrate and ammonium chloride. The A773 wildtype and the *Ccg-1* promoted strain, G11, were inoculated on standard minimal media (containing 35 mM nitrate and no ammonium). The LQ-1 wildtype and the *niiA*-promoted strain, rss3, were inoculated on an inducing medium containing 10 mM sodium nitrate and no ammonium chloride, a non-inducing medium containing 10 mM sodium nitrate and 0.2 mM ammonium chloride, and a repressing medium which contained no sodium nitrate and 4 mM ammonium chloride. The cultures were incubated for two days before assaying the colony diameters. From day three to day seven, the diameter of the fungal strains was measured at approximately the same time of day using a ruler and cm units. In the comparison of the wildtype, A773, to the G11 strain, and of the wildtype, LQ-1, to the rss3 strains, colony diameters were measured at approximately 11 a.m. and 2 p.m., respectively. Colony diameter was measured across two dimensions and averaged to account for colonies that were not perfectly round. To determine if there was a significant difference in the growth of the colonies between the wildtypes and the Lifeact expressing strains, a two-tailed student's T-test assuming unequal variances was performed ($p<.05$).

Time-lapse microscopy

All time-lapse image acquisition was performed using an Olympus BX51 fluorescence microscope outfitted with an Olympus DSU (http://www.olympus-ims.com/en/microscope/) and a Hamamatsu Orca ER camera (http://sales.hamamatsu.com/) interfaced with a microcomputer running SlideBook 5.0.0.25 x32 (Intelligent Imaging Innovations, Inc.). A Prior shutter (Prior

Scientific, Inc.) positioned in each light path was triggered by the SlideBook software. The shutter was used to create a dark period to avoid photo-toxicity to the cells. The reporter used was Lifeact, an actin binding protein domain fused to either a green fluorescence protein (GFP) or red flourescence protein (RFP).

The *Ccg-1* promoted Lifeact-GFP strain, G-11, was incubated on fully supplemented standard solid minimal medium for approximately 21 hours under constant light at 28°C to image for mature developmental stages, such as branch formation and septation. Constant light was used to prevent variation in actin expression due to circadian rhythms promoted by *Ccg-1*. The *niiA* promoted Lifeact-RFP strain, rss3, was incubated on a fully supplemented solid minimal medium containing 10 mM sodium nitrate for approximately 21 hours at 28°C to image for mature stages of development. Cultures of the *niiA* promoted Lifeact-RFP strain, rss3, were incubated on a fully supplemented standard minimal medium for approximately 5 hours at 32°C when imaging for conidial germination. Cells were imaged on agar blocks using standard methods (Frietag et al., 2004).

Imaging of conidial and hyphal anastomosis

Conditions for the imaging of conidial anastamosis and hyphal anastamosis in *A. nidulans* were found to be deficient in both macronutrients, nitrate and glucose. A 10^6 spore solution of the *Ccg-1* promoted Lifeact-GFP strain, G-11, or the *niiA* promoted Lifeact-RFP strain, rss3, was spot inoculated on fully supplemented solid minimal medium containing 10 mM sodium nitrate and 7 mM glucose. The cultures were incubated under constant light for approximately 12 hours

at 28°C when imaging for conidial anastomosis and for approximately 72 hours at 28°C when imaging for hyphal anastomosis.

Subapical actin web (SAW) and apical actin array (AAA) analysis

Hyphae were chosen for imaging based on the following criteria: the hyphae were undergoing growth, a subapical collar of actin patches was present (as described, Upadhyay and Shaw 2008), and whether or not the hyphae possessed a subapical actin web (SAW) or an apical actin array (AAA). Using the ruler tool in SlideBook, the distance between the hyphal tip and the SAW was measured. The growth rate was recorded by using the ruler tool to measure the distance each hyphae had grown and dividing it by the duration of the time between each frame. A two-tailed student's T-test assuming unequal variances was then performed to determine if there was a significant difference between the growth rates of hyphae possessing either the SAW or the AAA ($p<.05$).

CHAPTER III

RESULTS

Acquisition of the Lifeact expressing strains

Insertion of both expression vectors, *Ccg-1* and *niiA,* in the Lifeact expressing GFP and RFP strains (G11 and rss3, respectively) was verified by Laura Quintanilla using microscopic observation and PCR (Berepiki, et al., 2010; Quintanilla, 2013). Under microscopic observation, the *Ccg-1* promoted strain, G11, expresses for Lifeact when exposed to light. The Lifeact strain, rss3, promoted by the regulatory expression vector, *niiA,* was observed under three different conditions: inducing, low inducing, and repressing. On the inducing medium, the rss3 strain is observed to have a high level of expression for actin in comparison to the low inducing medium. The rss3 strain had no expression for actin on the repressing medium.

Fitness tests

A colony diameter comparison of the wildtype, A773, to the Lifeact expressing GFP strain, G11, revealed that the average growth of the G11 strain is within the standard error of the average growth of the wildtype over the five day period (Figure 1). However, a two-tailed student's T-test revealed a significant difference in the growth rates between the two strains from Day 4 to Day 7 ($p<.05$). When comparing the average conidia production of the wildtype to the G11 strain, it was determined that the G11 strain produced slightly more conidia than that of the wildtype (Figure 2). A two-tailed student's T-test revealed that there was not a significant difference in the number of conidia produced by the two strains ($p<.05$).

The colony diameter comparison of the wildtype, LQ-1, to the Lifeact expressing RFP strain, rss3, revealed that the average growth of the RFP strain is within the standard error of the average growth of the wildtype on the inducing, low inducing, and repressing media (Figure 3)(Quintanilla, 2013). However, a two-tailed student's T-test revealed a significant difference between the growth of the wildtype and the rss3 strain on the inducing and repressing media ($p<.05$). A conidial production comparison of the wildtype, LQ-1, to the Lifeact-RFP strain, rss3 determined that the wildtype produced slightly more conidia than rss3 in every condition (Figure 4). A two-tailed student's T-test revealed that there was not a significant difference in the number of conidia produced by the two strains when grown on the three types of media ($p<.05$).

Endocytic subapical collars are required for polarized growth

The endocytic subapical collar has been observed in all actively growing hyphae in both the *Ccg-1* and the *niiA* promoted Lifeact expressing GFP and RFP strains (Figure 5). The collar is composed of cortical actin patches which localize approximately 2 µm distal from the hyphal tip (Quintanilla, 2013). Actin cables are also present and appear to be associated with the Spitzenkörper, where it is likely that nucleation from the formin is occurring. Hyphae that possess an endocytic subapical collar grow normally in a polar direction. Hyphae, which have been observed to lose the endocytic subapical collar during development, swell at the tip and begin to grow abnormally (Figure 6). Polarized growth is restored upon the formation of the collar.

Contractile actin rings (CARs) appear prior to septation and branch formation

Septation

During septa formation, actin is documented to localize at the septation site (Figure 7; Figure 8). Actin cables move dynamically to a centralized area of the aseptae hyphae. The filamentous cables then organize to form a contractile actin ring (CAR) and septa formation is initiated. The actin ring forms a bow-like structure, with higher levels of expression for actin along the periphery of the tubular hyphae. As septa formation continues, actin expression increases towards the center of the cell. Once the septum is fully formed, actin cables migrate away from the septation site and the actin localization contracts down to a single point.

Branch formation

Actin localization and dynamics have been documented in the formation of hyphal branches in the Lifeact expressing RFP strain, rss3 (Figure 9; Figure 10). Actin cables and patches first localize to the site where a new branch will form. The actin cables organize into the CAR and branching is initiated. As the branch develops, a number of the actin cables form the apical actin array (AAA) that localizes at the apex of the growing cell. Once the branch initial is established, the AAA retracts and relocates within the parent hyphae (Figure 11). The hyphal branch then gains an endocytic subapical collar and continues to grow and develop in a normal, polarized direction. This is similar to what has been demonstrated in other mature, growing hyphae.

Actin cables localize to the site of germ tube formation

Actin cables are present but disorganized in dormant conidia (Figure 12). As the conidium germinates, it swells at the site of polarization. Actin cables localize and polarity is established. The germ tube is formed and continues to develop, while simultaneously actin cables relocate into the site of new growth. As the germ tube grows, actin cables form the AAA. During germ

tube septation, actin cables localize to the nascent septation site and begin to constrict by forming the CAR (Figure 13). The CAR reduces to a point of localization as the septum is formed. Eventually, the actin dissipates from the newly formed septum.

Actin dynamics during conidial and hyphal anastomosis

Conidial anastomosis

Asexual conidia in close proximity fuse in the Lifeact expressing GFP strain, G11 (Figure 14). The conidial anastomosis tube (CAT), or fusion bridge, is morphologically distinct from germ tubes or hyphae. The fusion bridge occurs approximately 90° from the germ tubes on each conidium. Actin cables localize at the area where anastomosis is about to occur. Once the connection is established, actin cables migrate into the fusion bridge. A direct connection, morphologically aseptae, is formed between the two condia.

Hyphal anastomosis

Two hyphae fuse in an anastomosis event in the Lifeact expressing RFP strain, rss3 (Figure 15). Similar to what was observed in the cell fusion between conidia of the Lifeact expressing GFP strain, G11, the fusion tube is morphologically distinct from germ tubes or hyphae. The fusion occurs laterally, distal from the hyphal apices. In each hypha, actin cables localize at the site where fusion is initiated. The connection is established and simultaneously actin cables migrate into the fusion bridge. It is unclear if actin is exchanged between the hyphae once anastomosis has occurred.

Apical actin arrays (AAAs) and subapical actin webs (SAWs)

F-actin structures, AAAs and SAWs, have both been documented in the Lifeact expressing RFP and GFP strains, rss3 and G11. In a comparative analysis, a total of 60 actively growing hyphae were observed based on the presence of a AAA or SAW (Table 2).

The SAW structure was found in 36.7% of the hypha observed. The average localization of the SAW is approximately 6.2 μm distal to the tip, with a standard deviation of 2.1 μm. Digital images of the SAW in various individual hyphae can be found in Figure 16. The SAW is composed of actin cables, which localize to form a mesh-like structure in the subapical region of the hyphae. The SAW appears to exhibit different dynamic patterns when compared to the AAA. The proximal face is dynamic, with cables polymerizing and depolymerizing toward the tip of the hyphae. In contrast, the distal face is relatively stable. When observing actin dynamics throughout the mycelia, SAWs maintain a similar relative distance in the majority of the growing cells (Figure 17).

The AAA structure was found in the apex of 63.3% of the hypha observed. Like that of the SAW structure, the AAA is composed of actin cables organizing into a mesh-like stucture (Figure 18). In contrast to the SAW, the proximal face of the structure within the apex is stable, whereas the side distal to the apex is dynamic. The AAA structures maintains a consistent relative distance in the majority of the growing cells (Figure 19).

The average growth rate of the hypha possessing a SAW is 0.7 μm per minute with a standard deviation of 1.0 μm/min (n=22). In hypha where the AAA is present, the average growth rate is

0.4 μm/min. The standard deviation is 0.2 μm/min (n=38). A two-tailed student's T-test assuming unequal variances was performed to compare the growth rate data (Table 3). There was no significant difference between the growth rates of hyphae possessing a SAW or those cells with the AAA ($p<.05$).

CHAPTER IV

DISCUSSION

Lifeact-GFP and -TagRFP have been shown to be reliable markers for expression of F-actin assemblages in filamentous fungi (Riedl, et al., 2008). However the fitness tests performed in this study using both the Lifeact constructs, G11 and rss3, were inconclusive in declaring that Lifeact has no negative effects on fitness. When comparing the *Ccg-1* promoted Lifeact-GFP strain, G11, to the wildtype, A773, there was statistical significance in the growth rates indicating that fitness is affected. On the contrary, the conidial production comparison resulted in no significant difference between the two strains. These results suggest that the fitness of the G11 strain is at least partially effected by expression of Lifeact. This is not surprising given the expression of a foreign construct that decorates the entire actin cytoskeleton of the organism. It does require however, that the interpretation of these results needs to be carried out with the fitness effects in mind.

In the colony diameter comparison of the *niiA* promoted Lifeact-TagRFP strain, rss3, to the wildtype, LQ-1, the fitness of the fungus varied with the type of media utilized. Based on the statistical analysis, the fitness of the Lifeact strain was significantly different when grown on the inducing and repressing media. Although like that of the G11 strain, fitness was not statistically different based on the conidial production of rss3 and LQ-1. Conclusively, it appears that Lifeact may have a negative effect on growth rate but does not affect conidial production. Given that conidiation is essential to the lifecycle of the organism, coupled with the observation that conidiation is not effected by lifeact expression, any fitness effects are likely to be minimal.

This research documented actin dynamics and localization in the polarized growth of the hyphae. Endocytic subapical collars were observed in all actively growing hyphae. When the subapical collar is diminished, tip swelling and abnormal elongation proceeds. This confirms previous studies on the necessity of the subapical collar in maintaining normal growth patterns in filamentous fungi. Furthermore, these results indicate that the actin localization reported by Lifeact is physiologically relevant (Berepiki, et al., 2010; Shaw, et al., 2011; Delgado, et al., 2011).

In the microscopic observation and time-lapse imaging of the Lifeact expressing RFP strain, rss3, CARs appeared prior to septation and branch formation. During both developmental stages, actin cables coalesce around the region of new growth, organizing to form the CAR. This data is consistent with the previous descriptions of actin protein involvement in septa and branch formations in *A. nidulans* and *N. crassa* (Berepiki et al., 2010; Delgado-Álvarez et al., 2010; Quintanilla, 2013). In addition, the AAA is present during the establishment of branches in the lateral region of the hyphae. Similar conclusions were documented in the involvement of the AAA in the branch formation of *N. crassa* (Lichius, et al., 2011).

The AAA was also present during conidial germination. Prior to the establishment of polarity, the conidium is spherical with actin patches, but not cables, present within the cell. Upon conidial germination, the conidium began to swell and actin cables localized at the site where polarity is established. The actin cables coalesce to form the AAA as the formation of the germ tube is initiated. The AAA migrates to the apex as the germ tube grows and develops. This

process of germ tube development coincides with previous documentation of conidial germination in *A. nidulans* (Takeshita and Fischer, 2011). There has been prior studies of actin involvement in hyphal morphogenesis during conidial germination in filamentous fungi, including *A. nidulans* and *N. crassa* (Momany, 2002; Takeshita and Fischer, 2011; Berepiki, et al., 2011; Quintanilla, 2013). However, there was a limited understanding of actin dynamics exhibited in the germ tube formation of *A. nidulans.* The results of this study show the correlation between actin dynamics in both the fungal species, *A. nidulans* and *N. crassa.* This evidence supports the theory that actin patterns in conidial germination are conserved amongst different species of filamentous fungi.

It was documented that actin cables will form the CAR during germ tube septation in *A. nidulans*. Prior to septum formation, actin cables localized to the septation site on the germ tube. The localized actin cables form the CAR and septa formation is initiated. The CAR remains persistent at the site until the septum is fully developed. This data coincides with the actin localization patterns observed in hyphal septation (Berepiki, et al., 2010; Harris, 2001). Before and during conidial septation, a secondary germ tube was not initiated. These data are consistent with previous documentation on the process of conidial germination in *A. nidulans* (Takeshita and Fischer, 2011).

This research is the first of its kind to present live cell imaging data of cytoskeletal dynamics during conidial and hyphal anastomosis in *A. nidulans.* Therefore, the understanding of these phenomena in *A. nidulans* had been seriously lacking and required further investigation. Microscopic observation and time-lapse imaging revealed asexual conidia in close proximity

undergo anastomosis, establishing a connection through the formation of a fusion bridge. The conidial anastomosis tube (CAT), or fusion bridge, was morphologically distinct from germ tubes or hyphae due to their reduced diameter. This observation coincides with previous research on CAT formation in *N. crassa, C. lindemuthianum* and other filamentous fungal species (Roca, et al., 2005; Krijgsheld, et al., 2012).

Previous studies on actin dynamics during conidial anastomosis had only been performed for the filamentous fungal species, *N. crassa* (Read, et al., 2012). It was documented that actin cables first localized at the area where anastomosis was about to occur. Once the connection was established, actin cables migrated into the fusion bridge. A direct connection was formed between the two conidia. This would allow for the transfer of cytoplasm and other cellular components, such as nuclei, as well as the exchange of water and nutrients between the two cells. These results are similar to the data reported in the live-cell imaging of actin dynamics during CAT formation in *N. crassa.* Continued research is needed to compare or contrast CAT formation of *A. nidulans* to other filamentous fungi.

There has been evidence that the development of anastomosis tubes between hyphae is mediated by actin related genes conserved in *S. cerevisiae* and *N. crassa* (Glass, et al., 2004). In addition, hyphal anastomosis has been thoroughly documented in *N. crassa.* However, live-cell imaging of actin during hyphal fusion or anastomosis in filamentous fungi has never been performed. Therefore the results of this study are novel in the characterization of actin dynamics and localization during this developmental stage in filamentous fungi, particularly *A. nidulans.* The data shows that actin cables localized at each fusion bridge in the corresponding hyphae. Once

the connection is established, the actin cables migrated into the fusion bridge and appeared to localize directly to the site where each cell wall was being digested. At that point, the formerly polarized bridges begin to grow isotropically. The actin cables continued to localize within the fusion bridge even after the formation of the bridge had been completed and the cell walls had been fully digested. The development of hyphal anastomosis appears to be conserved amongst both the fungal species, *A. nidulans* and *N. crassa* (Hickey, et al., 2002; Glass, et al., 2004). Because these observations are the first to be documented, a comparison of actin dynamics during the hyphal fusion of both species cannot be implemented. Although actin may not be required for the maintenance of polarization throughout the entire process of anastomosis, the protein does play another vital role in establishing the connection between two hyphae. More research is needed to develop a better understanding of the actin requirement during hyphal anastomosis in *A. nidulans* and other filamentous fungi.

The SAW and AAA are actin structures that have been documented in the hyphae of *A. nidulans.* Both the SAW and the AAA are constituted from a mesh-work of actin cables. The actin cable dynamics, however, differed in each structure. The SAW appears to exhibit patterns in which the proximal face of the structure closest to the apex is dynamic, with cables polymerizing and depolymerizing towards the tip of the hyphae. In contrast, the distal face was relatively stable. This conclusion is correlative to previous results of SAW dynamics reported in *A. nidulans* (Quintanilla, 2013). The SAW was found to be located in the subapical region, on average approximately 6.2 μm distal from the tip.

The AAA, found in the apical region of the hyphae, was observed to demonstrate actin dynamics which were antithetical to that of the SAW. In comparison, the proximal face of the AAA structure within the apex was stable, whereas the distal face was dynamic. The AAA was often observed during the formation of branches and conidial germination. These observations are consistent with the AAA structural dynamics recovered in both *A. nidulans* and *N. crassa* (Lichius, et al., 2011; Quintanilla, 2013). Based on the conservation of the AAA in both species of filamentous fungi, it is theorized that the AAA plays a major role in the initiation of hyphal morphogenesis.

Following a statistical analysis, it was determined that there is no significant difference between the growth rates of hyphae possessing the two different structures ($p<.05$). This is disparate from previous studies in the comparison of hyphal growth rates in the presence of the AAA or SAW (Quintanilla, 2013). It is possible that the sample size was a limiting factor when making this conclusion. More evidence is needed to understand the effects of the SAW and AAA on the growth rate of the fungus. In addition, the localization patterns of each structure across the entire mycelium still requires further inquiry. Due to the fact that the SAW and AAA are so similar in composition, it is unclear whether the two structures are distinct or synonymous in nature.

CHAPTER V

CONCLUSION

The aim of this study was to identify actin dynamics and localization in the filamentous fungus, *A. nidulans.* Actin is a vital protein which is conserved in all higher eukaryotes. The fluorescent marker, Lifeact, was used to label actin cables and patches. Actin cables and patches were present during each stage of development, including hyphal growth, septation, branch formation, conidial germination, and conidial and hyphal anastomosis. Continued studies of conidial and hyphal fusion is needed to fully understand anastomosis in *A. nidulans.* Other actin structures were documented, including the SAW and the AAA. Further research is needed to characterize the roles of these structures. The laboratory is currently creating a construct that will express for the Hex1 protein, as well as Lifeact-GFP (Quintanilla, 2013). This will allow us to observe actin dynamics in relation to woronin bodies. By understanding more about the actin protein in *A. nidulans,* we may find ways of controlling fungal diseases of plants and animals.

REFERENCES

Adams, T. H., Wieser, J. K., & Yu, J.-H. (1998). Asexual sporulation in *Aspergillus nidulans*. *Microbiology and Molecular Biology Reviews, 62*(1), 35-54.

Anwar, M. M., Croft, J. H., & Dales, R. B. (1993). Analysis of heterokaryon incompatibility between heterokaryon-compatibility (h-c) groups R and GL provides evidence that at least eight het loci control somatic incompatibility in *Aspergillus nidulans*. *Journal of General Microbiology, 139*(7), 1599-1603.

Berepiki, A., Lichius, A., & Read, N. D. (2011). Actin organization and dynamics in filamentous fungi. *National Reviews in Microbiology, 9*(12), 876-887.

Berepiki, A., Lichius, Alexander, Shoji, Jun-Ya, Tilsner, Jens and Read, Nick. D. (2010). F-actin dynamics in *Neurospora crassa*. *Eukaryotic Cell, 9*(4), 547-557.

Delgado-Álvarez, D. L., Callejas-Negrete, O. A., Gómez, N., Freitag, M., Roberson, R. W., Smith, L. G., & Mouriño-Pérez, R. R. (2010). Visualization of F-actin localization and dynamics with live cell markers in *Neurospora crassa. Fungal Genetics and Biology, 47*(7), 573-586.

Freitag, M., Hickey, P. C., Raju, N. B., Selker, E. U., & Read, N. D. (2004). GFP as a tool to analyze the organization, dynamics and function of nuclei and microtubules in *Neurospora crassa*. *Fungal Genetics and Biology, 41*(10), 897-910.

Gabriela Roca, M., Read, N. D., & Wheals, A. E. (2005). Conidial anastomosis tubes in filamentous fungi. *FEMS Microbiology Letters, 249*(2), 191-198.

Glass, N. L., Jacobson, D. J., & Shiu, P. K. T. (2000). The genetics of hyphal fusion and vegetative incompatibility in filamentous ascomycete fungi. *Annual Review of Genetics, 34*(1), 165-186.

Glass, N. L., Rasmussen, C., Roca, M. G., & Read, N. D. (2004). Hyphal homing, fusion and mycelial interconnectedness. *Trends in Microbiology, 12*(3), 135-141.

Goode, B. L., & Eck, M. J. (2007). Mechanism and function of formins in the control of actin assembly. *Annual Reviews in Biochemistry, 76*, 593-627.

Harris, S. D. (2001a). Hyphal Growth *eLS*: John Wiley & Sons, Ltd.

Harris, S. D. (2001b). Septum formation in *Aspergillus nidulans*. *Current Opinions in Microbiology, 4*(6), 736-739.

Harris, S. D. (2008). Branching of fungal hyphae: regulation, mechanisms and comparison with other branching systems. *Mycologia, 100*(6), 823-832.

Hervas-Aguilar, A., & Penalva, M. A. (2010). Endocytic machinery protein SlaB is dispensable for polarity establishment but necessary for polarity maintenance in hyphal tip cells of *Aspergillus nidulans*. *Eukaryotic Cell, 9*(10), 1504-1518.

Hickey, P. C., Jacobson, D. J., Read, N. D., & Louise Glass, N. (2002). Live-cell imaging of vegetative hyphal fusion in *Neurospora crassa*. *Fungal Genetics and Biology, 37*(1), 109-119.

Ishikawa, F. H., Souza, E. A., Shoji, J.-Y., Connolly, L., Freitag, M., Read, N. D., & Roca, M. G. (2012). Heterokaryon incompatibility is suppressed following conidial anastomosis tube fusion in a fungal plant pathogen. *PLoS ONE, 7*(2), e31175.

Kasuga, T., & Glass, N. L. (2008). Dissecting colony development of *Neurospora crassa* using mRNA profiling and comparative genomics approaches. *Eukaryotic Cell, 7*(9), 1549-1564.

Krijgsheld, P., Bleichrodt, R., van Veluw, G. J., Wang, F., Müller, W. H., Dijksterhuis, J., & Wösten, H. A. B. (2013). Development in *Aspergillus*. *Studies in Mycology, 74*(1), 1-29.

Lichius, A., Berepiki, A., & Read, N. D. (2011). Form follows function – The versatile fungal cytoskeleton. *Fungal Biology, 115*(6), 518-540.

McCluskey, K. (2003). The fungal genetics stock center: from molds to molecules. *Advances in Applied Microbiology*, 52, 245–262.

Momany, M. (2002). Polarity in filamentous fungi: establishment, maintenance and new axes. *Current Opinions in Microbiology, 5*(6), 580-585.

Momany, M., & Hamer, J. E. (1997). Relationship of actin, microtubules, and crosswall synthesis during septation in *Aspergillus nidulans*. *Cell Motility and the Cytoskeleton, 38*(4), 373-384.

Norwood, F. L., Sutherland-Smith, A. J., Keep, N. H., & Kendrick-Jones, J. (2000). The structure of the N-terminal actin-binding domain of human dystrophin and how mutations in this domain may cause Duchenne or Becker muscular dystrophy. *Structure, 8*(5), 481-491.

Osherov, N., & May, G. S. (2001). The molecular mechanisms of conidial germination. *FEMS Microbiology Letters, 199*(2), 153-160.

Penzes, P., & VanLeeuwen, J.-E. (2011). Impaired regulation of synaptic actin cytoskeleton in Alzheimer's disease. *Brain Research Reviews, 67*(1–2), 184-192.

Quintanilla, L. A. (2013). Actin dynamics in *Aspergillus nidulans*. *Texas Digital Libraries (TDL), Thesis.*

Read, N. D., Goryachev, A. B., & Lichius, A. (2012). The mechanistic basis of self-fusion between conidial anastomosis tubes during fungal colony initiation. *Fungal Biology Reviews, 26*(1), 1-11.

Riedl, J., Crevenna, A. H., Kessenbrock, K., Yu, J. H., Neukirchen, D., Bista, M., Bradke, F., Jenne, D., Holak, T. A., Werb, Z., Sixt, M., Wedlich-Soldner, R. (2008). Lifeact: a versatile marker to visualize F-actin. *Natural Methods, 5*(7), 605-607.

Seifert, J. (2008). Compartmentalized RhoA GTPases activation is associated with effects on actin binding proteins. *Texas Woman's University, Dissertation.* (3311823).

Shaw, B. D., Chung, D.-W., Wang, C.-L., Quintanilla, L. A., & Upadhyay, S. (2011). A role for endocytic recycling in hyphal growth. *Fungal Biology, 115*(6), 541-546.

Shinn-Thomas, J. H., & Mohler, W. A. (2011). New insights into the mechanisms and roles of cell-cell fusion. *International Review of Cell and Molecular Biology, 289*, 149-209.

Takeshita, N., & Fischer, R. (2011). On the role of microtubules, cell end markers, and septal microtubule organizing centres on site selection for polar growth in *Aspergillus nidulans*. *Fungal Biology, 115*(6), 506-517.

Upadhyay, S., & Shaw, B. D. (2008). The role of actin, fimbrin and endocytosis in growth of hyphae in *Aspergillus nidulans*. *Molecular Microbiology, 68*(3), 690-705.

Virag, A., & Griffiths, A. J. F. (2004). A mutation in the *Neurospora crassa* actin gene results in multiple defects in tip growth and branching. *Fungal Genetics & Biology, 41*(2), 213.

Xiang, X., & Plamann, M. (2003). Cytoskeleton and motor proteins in filamentous fungi. *Current Opinions in Microbiology, 6*(6), 628-633.

FIGURES

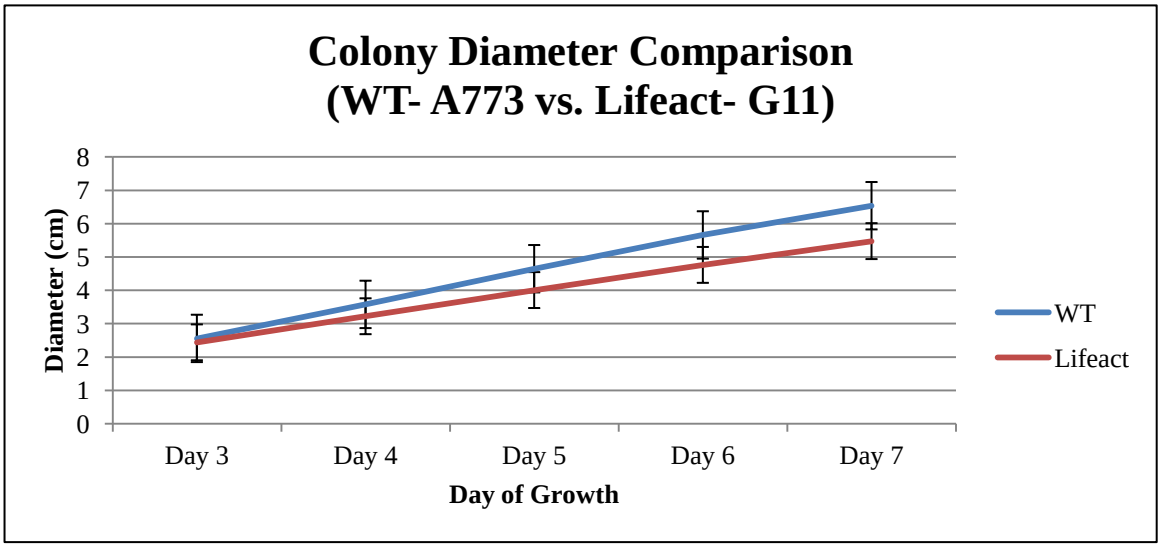

Figure 1. Comparison of colony diameter between wildtype, A773, and the Lifeact expressing GFP strain, G11. The graph shows the average colony diameter measurements over a 5 day period in two trials (n=6). The average growth of the G11 strain is within the standard error of the average growth of the wildtype (bars represent standard error). However, a two-tailed student's T-test revealed a significant difference in the growth rates between the two strains from Day 4 to Day 7 ($p<.05$). The data indicates that Lifeact expression promoted by *Ccg-1* affects fitness.

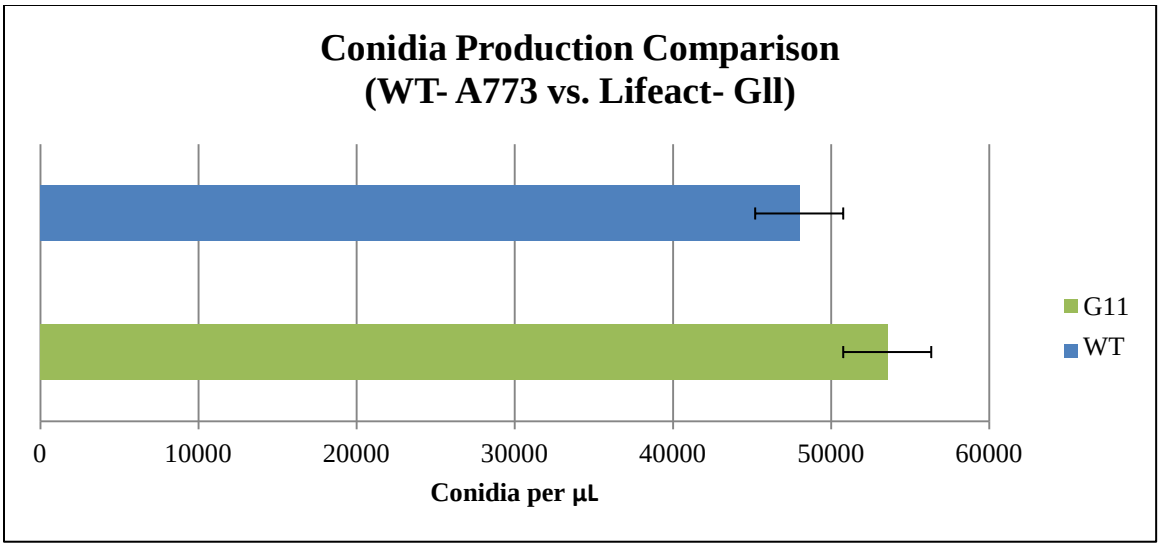

Figure 2. Comparison of conidia production between wildtype, A773, and the Lifeact expressing GFP strain, G11. The graph shows the average number of conidia per µL produced in two trials. The G11 strain produced a slightly higher concentration of conidia per µL than the wildtype. A two-tailed student's T-test revealed that there was not a significant difference in the number of conidia produced by the two strains ($p<.05$). This data indicates that the Lifeact strain, G11, is as fit as the wildtype (bars represent standard error).

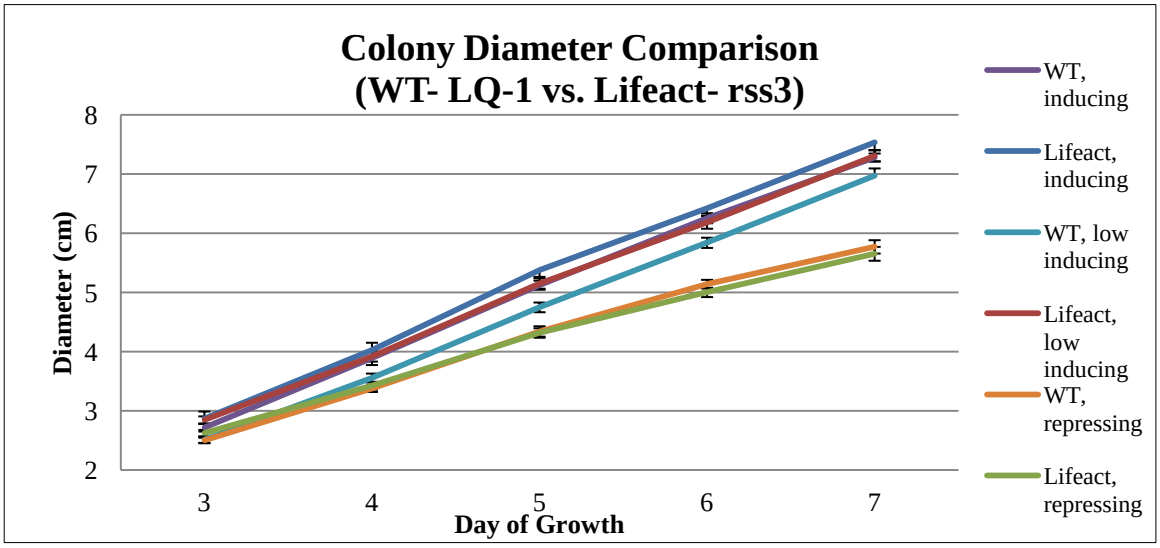

Figure 3. Comparison colony diameter between wildtype, LQ-1, and the Lifeact expressing RFP strain, rss3. The graph shows the average colony diameter measurements over a 5 day period in three trials (n=9). The average growth of the RFP strain is within the standard error of the average growth of the wildtype on the inducing, low inducing, and repressing media (bars represent standard error). However, a two-tailed student's T-test revealed a significant difference between the growth of wildtype and the rss3 strain on the inducing and repressing media ($p<.05$). This data indicates that Lifeact expression promoted by *niiA* does affect fitness under certain conditions. This data was recorded in concert with Laura Quintanilla (taken with permissions from Quintanilla, 2013).

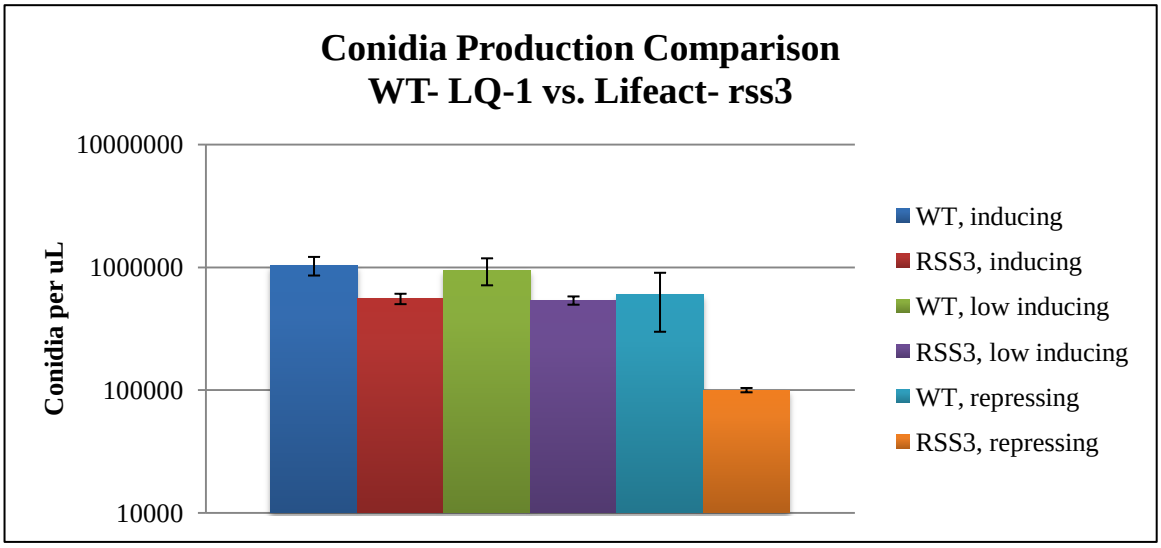

Figure 4. Comparison of conidial production between wildtype, LQ-1, and the Lifeact-RFP strain, rss3. The graph shows the average number of conidia per µL produced in three trials on the three different media types: inducing, low inducing, and repressing (n=9). The wildtype produced a slightly higher concentration of conidia per µL than the rss3 strain in every condition. However, a two-tailed student's T-test revealed that there was not a significant difference in the number of conidia produced by the two strains ($p<.05$) when grown on the three different types of media. This data indicates that the Lifeact strain, rss3, is as fit as the wildtype (bars represent standard error). This data was recorded in concert with Laura Quintanilla (taken with permissions from Quintanilla, 2013).

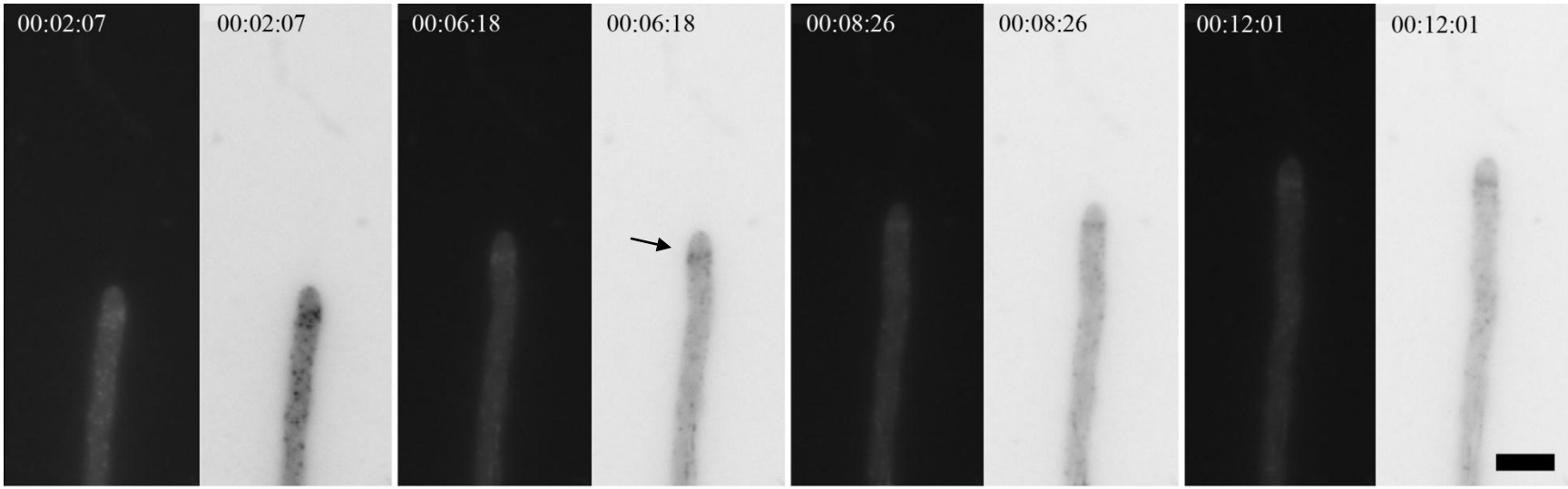

Figure 5. The endocytic subapical collar is present during hyphal growth. In panels 00:02:07 through 00:12:01 of the time sequence, an endocytic subapical collar is present in the growing hyphae (arrow). The hyphae is growing in a polarized manner. Bar=10 μm. Time=hh:mm:ss.

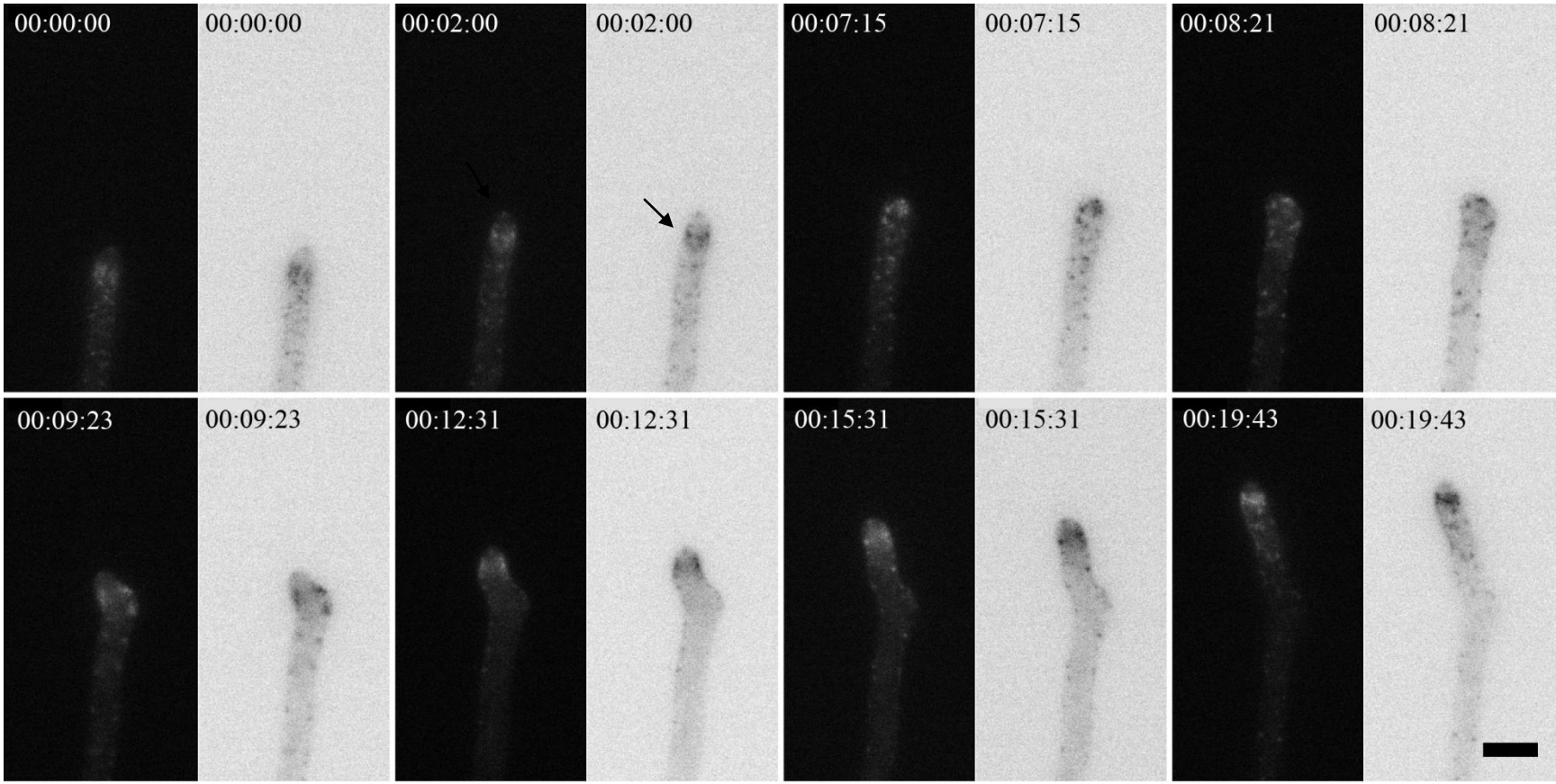

Figure 6. The endocytic subapical collar is required for the polarized hyphal growth. The time sequence demonstrates the importance of the subapical collar for hyphal growth. In panels 00:00:00 to 00:02:00, the subapical collar is present in the growing hyphae (arrow). In panels 00:07:15 to 00:08:21, polarized hyphal growth stops simultaneously with the loss of the collar. Polarized growth reinitiates in panel 00:09:23 with the formation of the collar. Polarized growth is continued in panels 00:12:31 through 00:19:43. Bar=10 μm. Time=hh:mm:ss

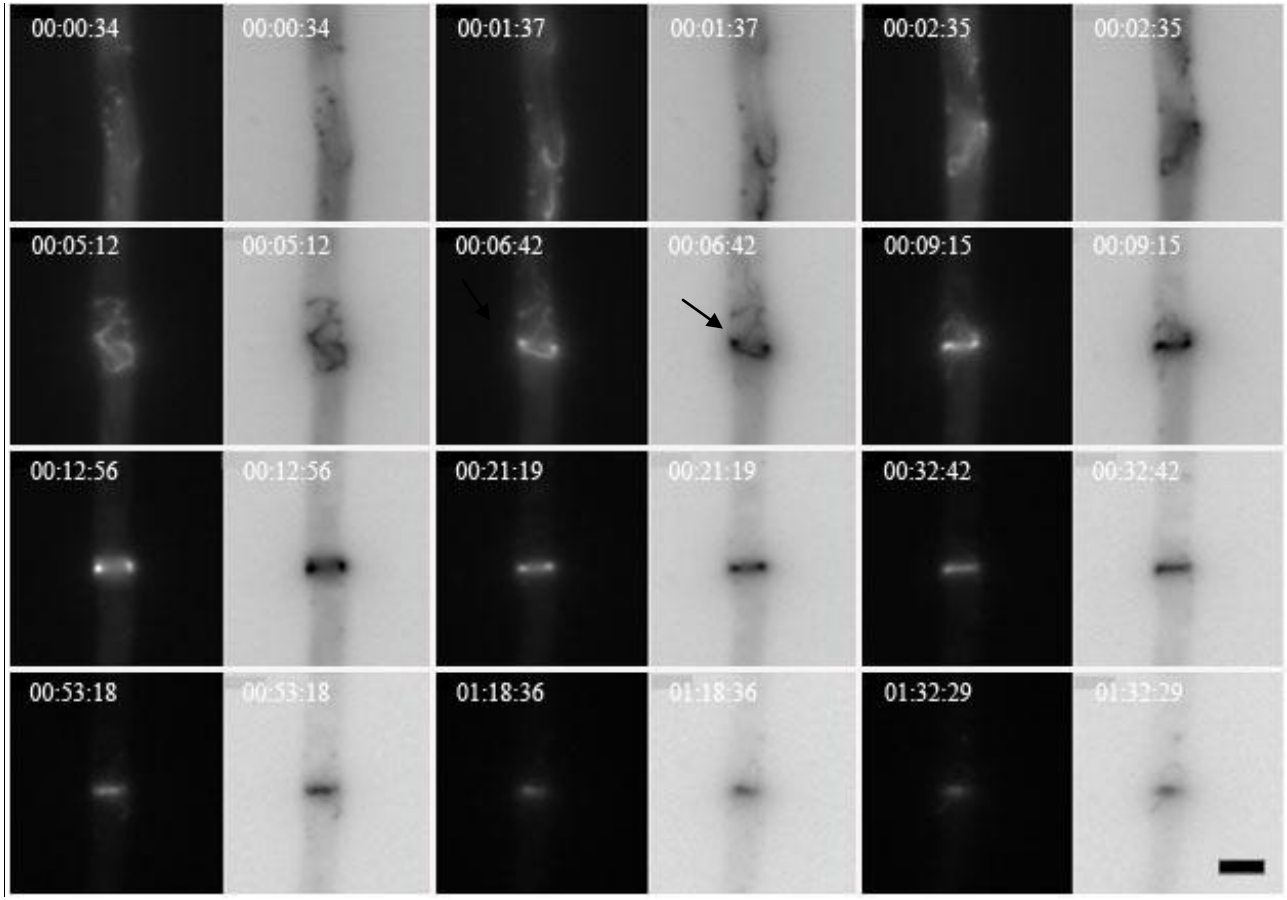

Figure 7. Actin localizes at a septation site during septum formation. In panels 00:00:34 to 00:05:12, actin cables dynamically locate in a centralized area of the hyphae. In panel 00:06:42, the cables form an actin ring (arrow). As seen in panels 00:09:15 through 00:21:19, the actin ring appears to then form a bow, with higher levels of actin along the periphery of the tubular hyphae. As septum formation continues, actin concentrates towards the center of the cell (panel 00:32:42) Once the septum has formed, the actin cables begin to leave the septation site and the actin is reduced down to a single point (panels 00:53:18 to 01:32:29). Bar=5 μm. Time=hh:mm:ss

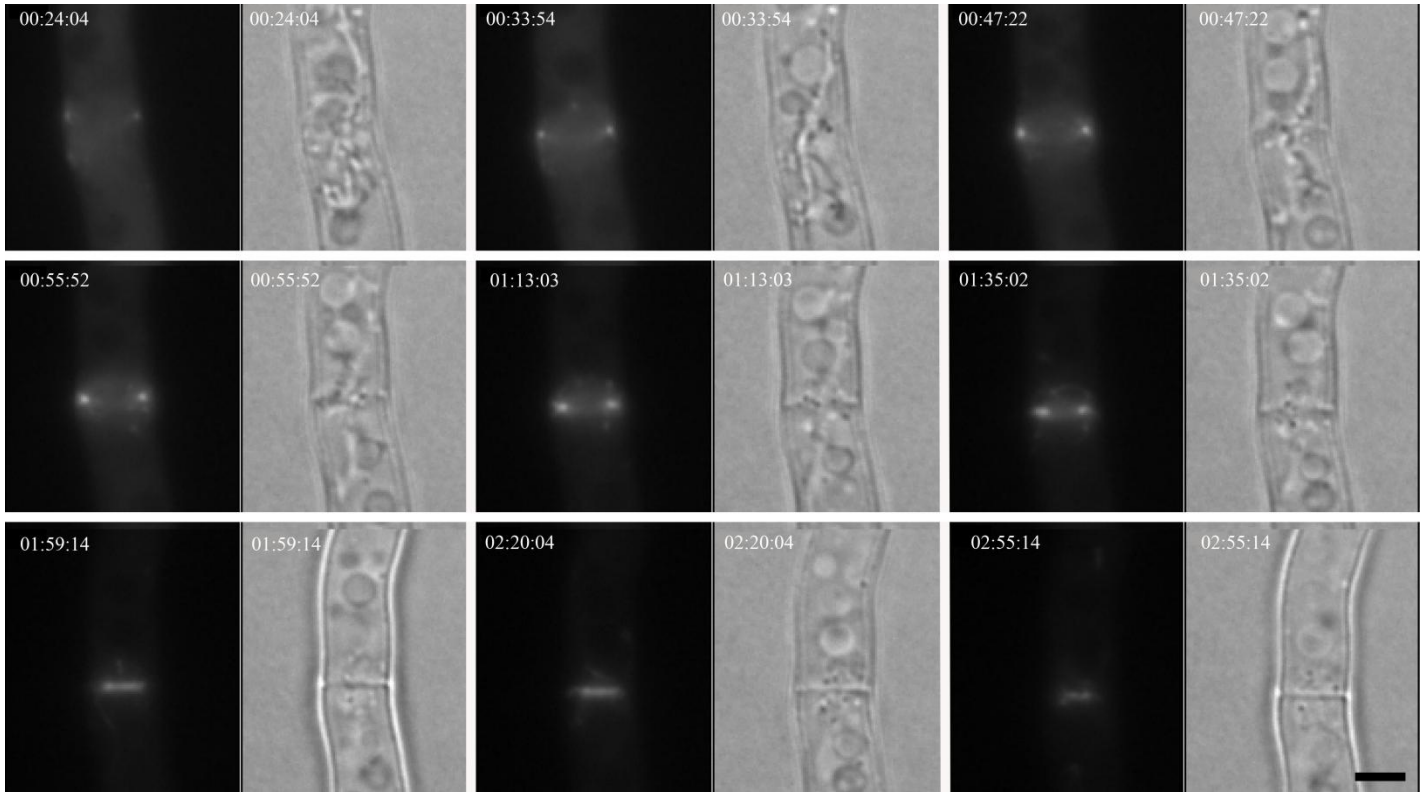

Figure 8. Actin localizes at a septation site during septum formation. The time sequence demonstrates the localization and the dissipation of actin during the formation of the hyphal septa. In panels 00:24:04 to 00:33:54, as actin cables begin to localize in a centralized area around the periphery of the tubular hyphae. The hyphae is observed to be aseptae with organelles free to move throughout the cytoplasm. In panels, 00:47:22 through 01:35:02, the filamentous cables have formed the actin ring and bow along the cellular walls of the hyphae. The bright field image shows the initiation of the septa formation. As seen in panel 01:59:14, as septa formation continues, actin expression increases towards the center of the cell. In panels 02:20:04 to 02:55:14, actin cables migrate away from the septation site once the septum is fully formed, and the actin dissipates down to a single point. Bar=2 μm. Time=hh:mm:ss.

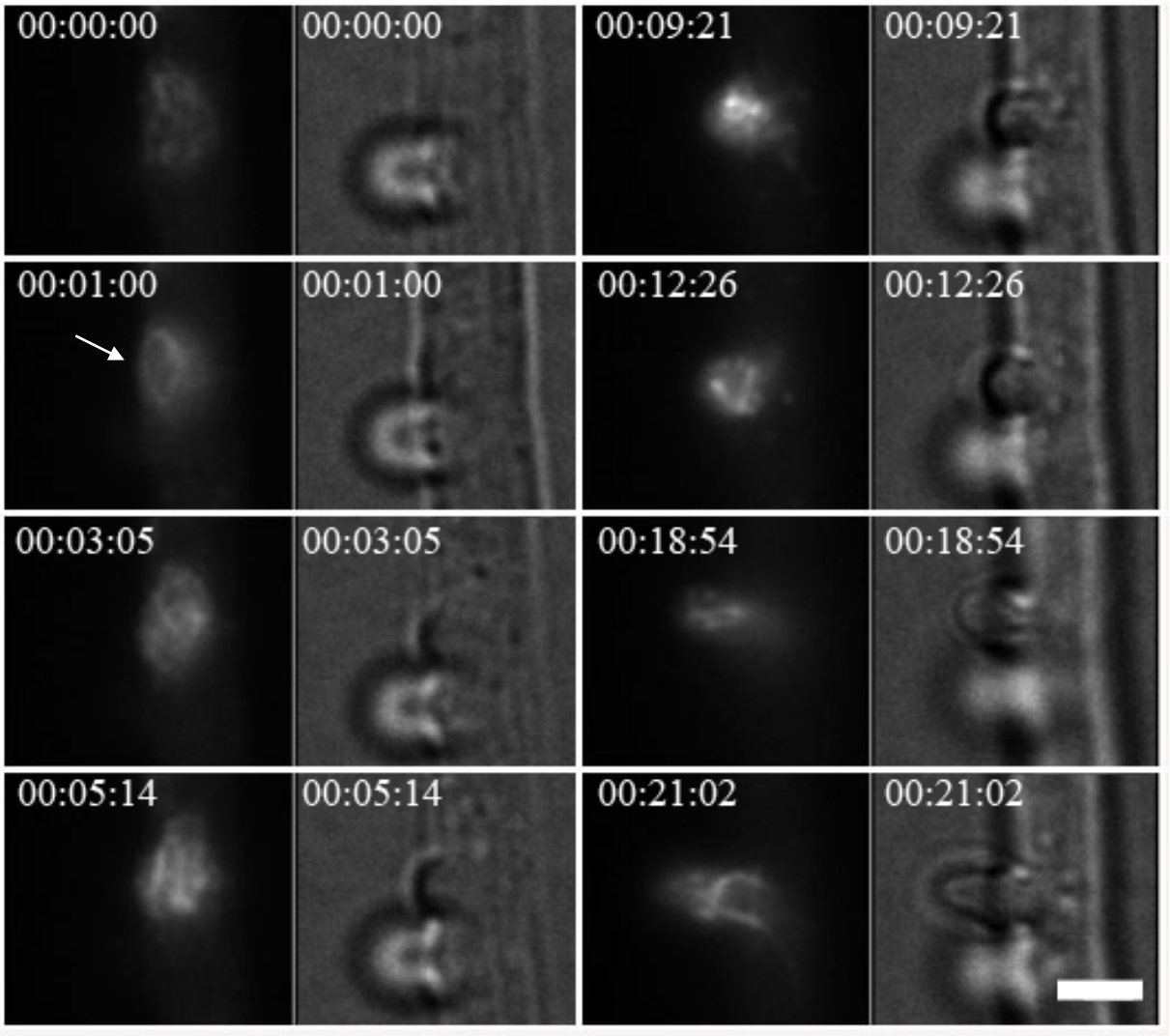

Figure 9. Actin cables localize to branch initials during branch formation. In panel 00:00:00, actin cables and patches organize to initiate the formation of a branch. The actin cables then localize and arrange to form the actin ring structure, as seen in panel 00:01:00 (arrow). In panels 00:03:05 through 00:12:26, the branch is beginning to develop on the lateral side of the fungal hyphae. By panels 00:18:54 to 00:21:02, actin cables, organized to form the AAA, have migrated to the inside of the branch as it continues to develop. Note that there is another branch site in the time sequence, positioned anterior to the secondary branch. Actin is absent from the branch and its development has ceased. This demonstrates the importance of actin in the continued growth and development of branching hyphae. Bar= 5 μm. Time=hh:mm:ss.

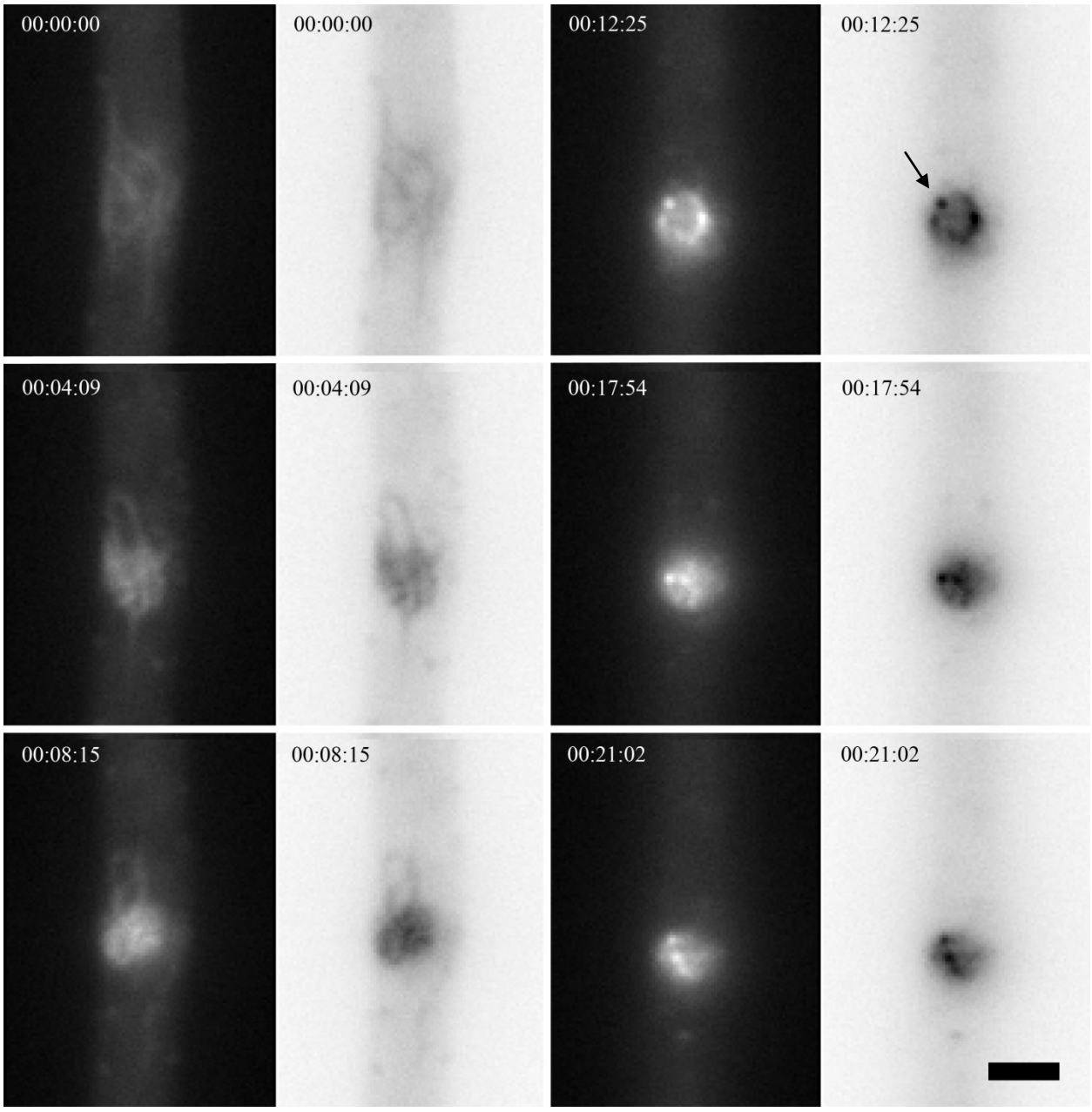

Figure 10. Actin localizes at branch site during branch formation. As documented in the time sequence, actin cables and patches localize to the site of branch formation. In panels 00:00:00 to 00:08:15, actin cables and patches begin to localize along the posterior side of the fungal hyphae. As documented in panel 00:12:25, the actin cables organize to form the actin ring structure (arrow). In panels 00:17:54 to 00:21:02, branch formation is initiated. Actin cables form the AAA, and migrates to the inside of the branch as it continues to develop. Bar=5 μm. Time=hh:mm:ss.

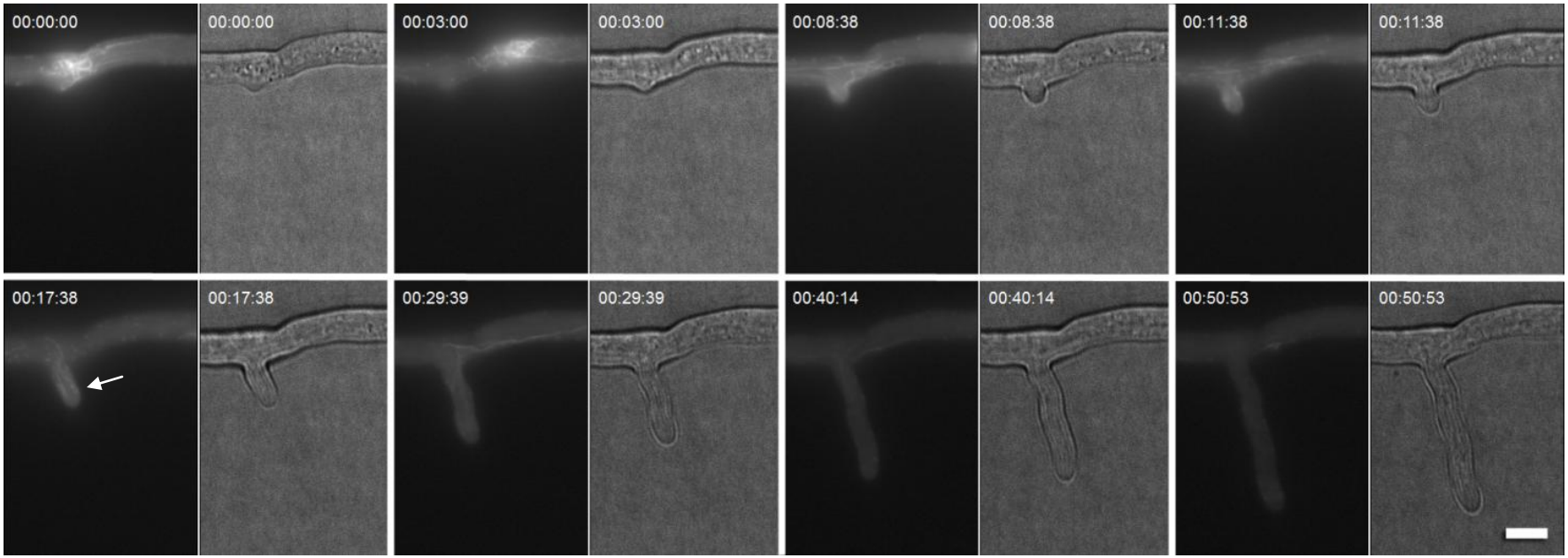

Figure 11. The endocytic subapical collar is formed upon the development of a hyphal branch (documented by Daisy Moncada-Monsivais). The time sequence demonstrates actin localization and dynamics during the growth and development of a hyphal branch. In panels 00:00:00 to 00:03:00, the actin cables that had localized during the formation of the branch, relocate away from the branch site. New cables localize to the inside of the growing cell and a endocytic subapical collar is formed distal to the hyphal tip, as seen in panels 00:11:38 through 00:50:53 (arrow). The branch continues to grow in a normal, polar direction, similar to what has been documented in other mature hyphae. Bar= 5 μm. Time=hh:mm:ss.

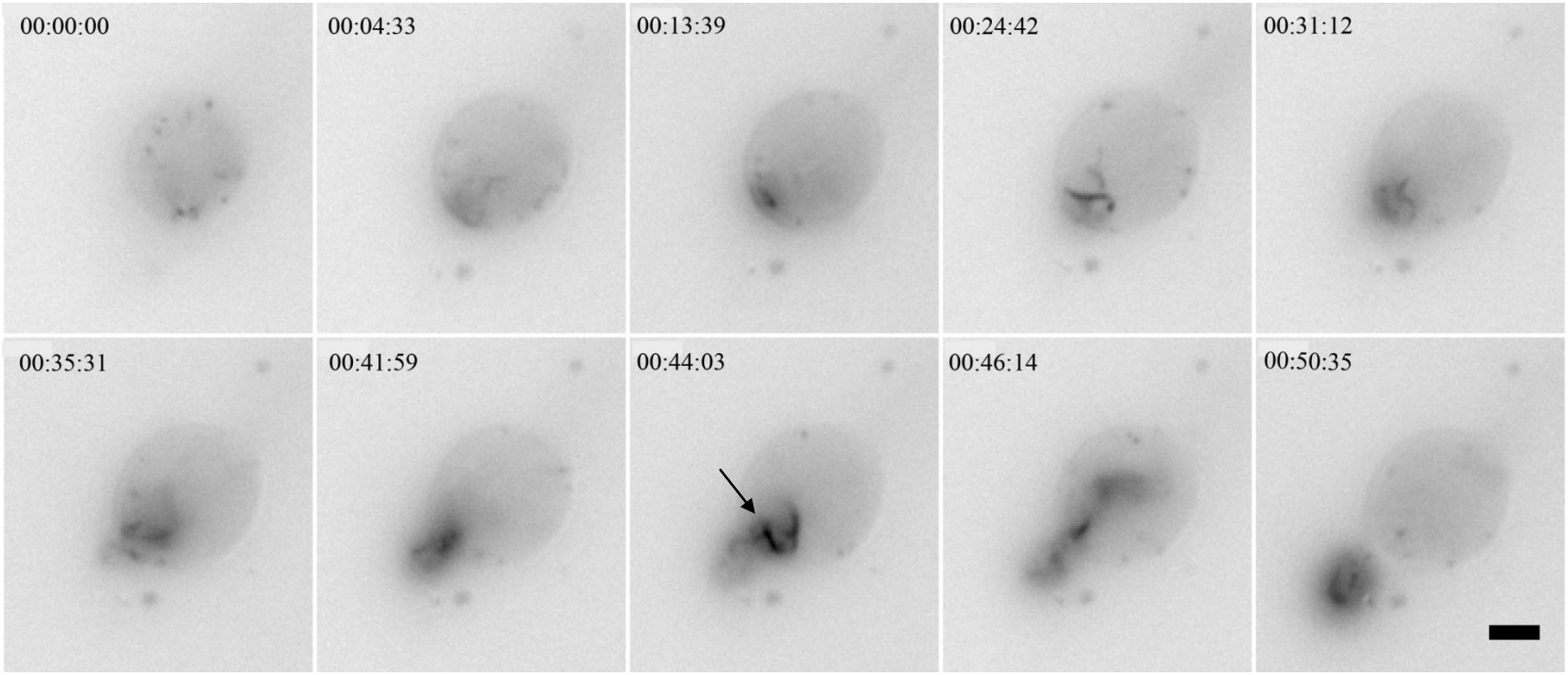

Figure 12. The apical actin array (AAA) is present during conidial germination. This sequence demonstrates actin localization and dynamics in a germinating conidium. In panel 00:00:00, actin patches, but not cables, are present in the conidium. The conidium is spherical and has no evidence of established polarity. In panels 00:04:33 through 00:31:12, actin cables begin to localize at the site of germination and polarity is established. The formation of the germ tube is initiated in panels 000:35:31 to 00:50:35. Actin cables form the AAA (arrow), which simultaneously migrates into the germ tube as it continues to develop. Bar=5 μm. Time=hh:mm:ss.

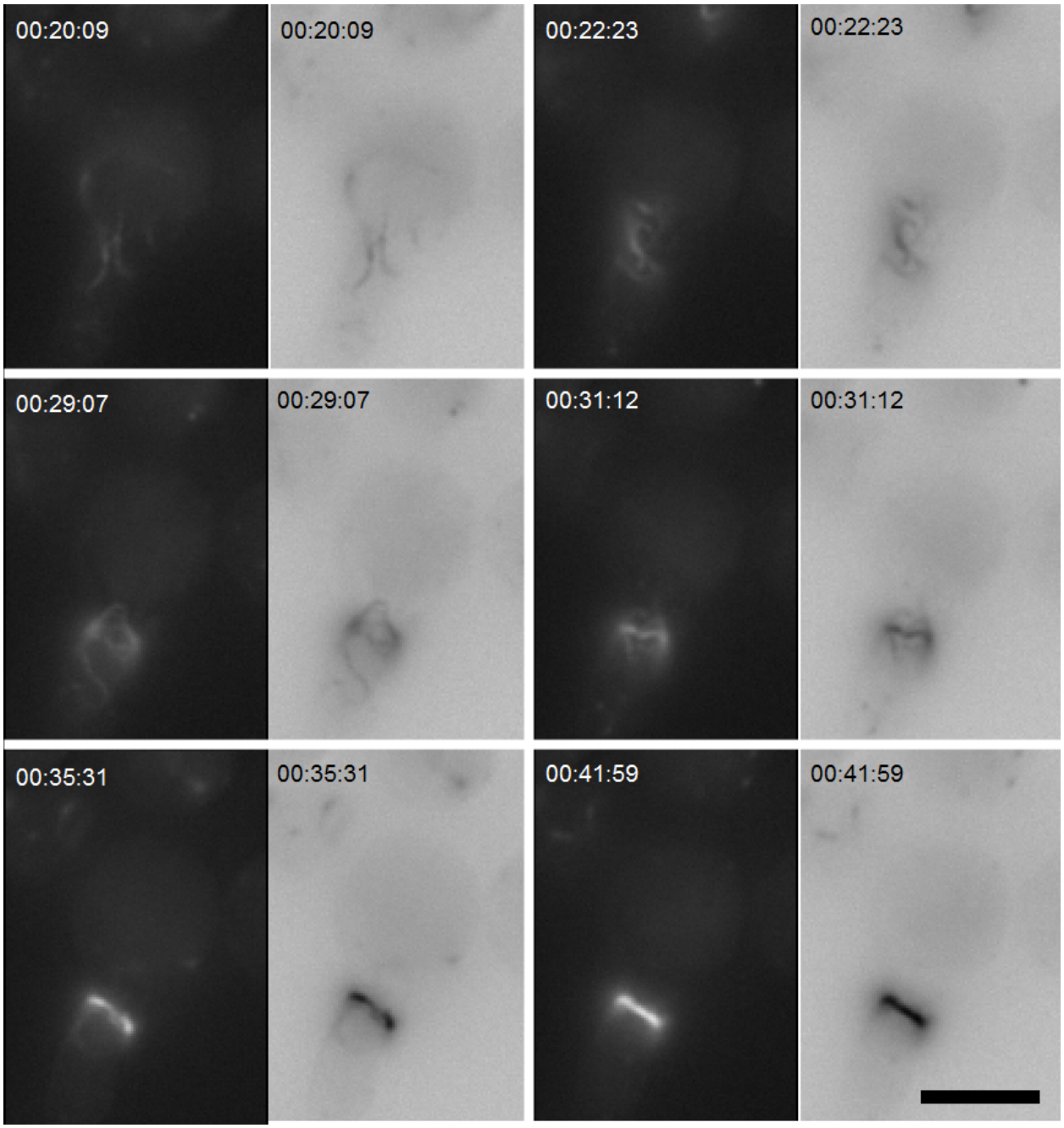

Figure 13. Actin cables form the contractile actin ring (CAR) during septation in a germling. In panels 00:20:09 through 00:29:07, actin cables localize to the site where septation is about to occur. In panels 00:31:12 through 00:35:31, the localized actin cables begin to the form the CAR. By panel 00:41:59, the CAR has fully formed and the septum continues to develop. This coincides with actin localization patterns observed in hyphal septation. Note that the conidium has not initiated secondary germ tube formation. These data are consistent with previous documentation on the process of conidial germination in *A. nidulans.* Bar=10 μm. Time=hh:mm:ss.

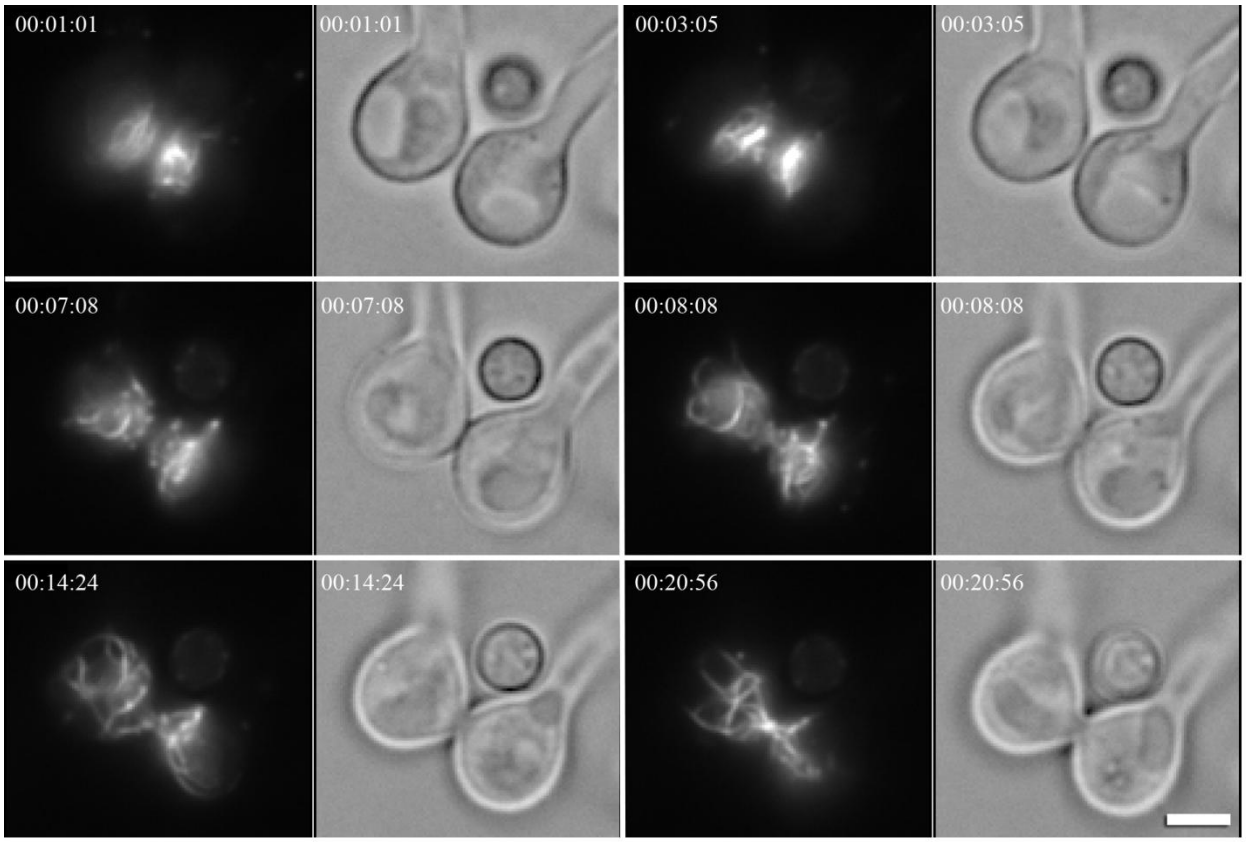

Figure 14. Actin localization and dynamics during conidial anastomosis fusion. Asexual conidia in close proximity undergo anastomosis, establishing a connection through the formation of a fusion bridge. The anastomosis tube, or fusion bridge, is morphologically distinct from germ tubes or hyphae, due to its reduced diameter. The fusion bridge occurs approximately 90° from the germ tubes on each conidium. In panels 00:01:01 through 00:07:08 actin cables localize to the polarization site where anastomosis is about to occur. Once the connection is established (panels 00:08:08 to 00:20:56), actin cables migrate into the fusion bridge. A direct connection, morphologically aseptae, is formed between the two condia. Bar=5 μm. Time=hh:mm:ss.

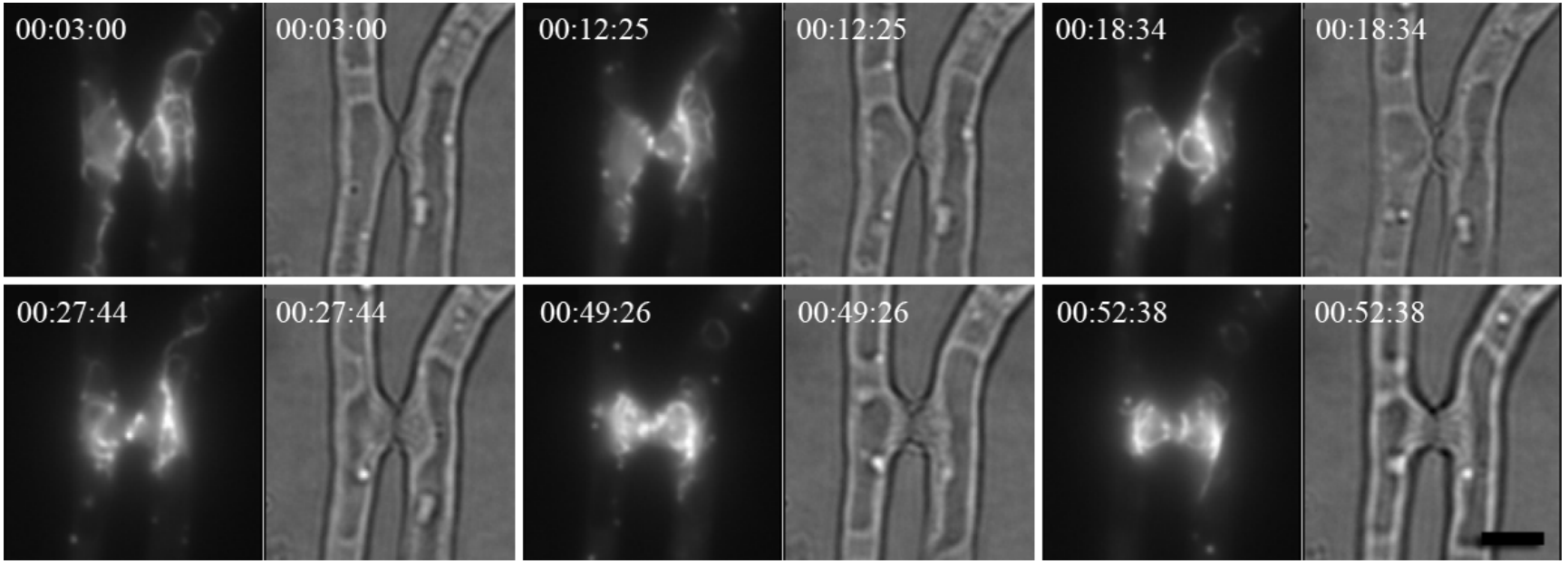

Figure 15. Actin localization and dynamics during hyphal fusion. Two hyphae fuse during an anastomosis event. In panels 00:03:00 through 00:18:34, actin cables localize to each polarized fusion bridge in the hyphae. As the connection is established in panel 00:27:44, polarization is lost and the fusion bridges begin to grow isotropically. Actin cables migrate into the fusion bridge and localize directly at the site where the cell walls are being digested. In panels 00:49:28 through 00:52:38, the formation of the fusion bridge is complete and the two cells have merged cytoplasm. Actin cables continue to localize to the fusion bridge. Bar=5 μm. Time=hh:mm:ss.

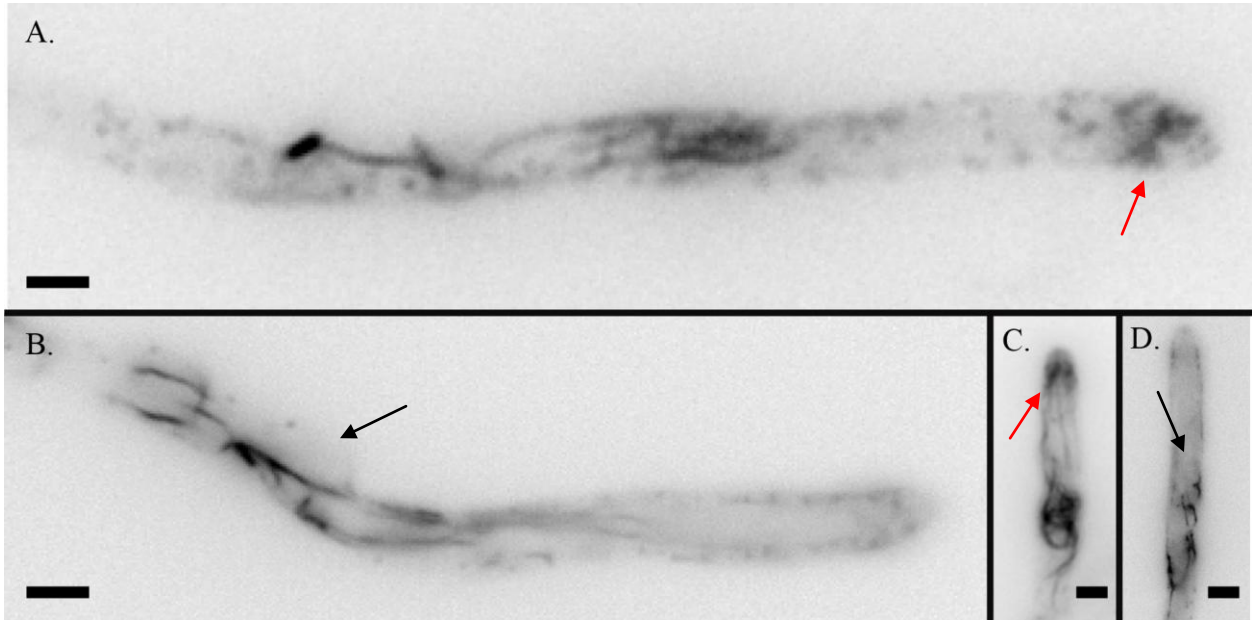

Figure 16. Actin cables localize to form the SAW in various hyphae (panels A., B., C. and D.). Actin cables organize to form a mesh-like structure, known as the SAW (black arrows indicated in panels B. and D.). The SAW is located in the subapical region of the hyphae and is an average of approximately 6.2 μm distal to the tip. Each hyphae presents a subapical collar, indicating that the cells are undergoing growth and development (red arrows indicated in panels A. and C.). The SAW is observed to display distinct dynamic patterns. The SAW has greater stability on the distal face with the greatest distance from the apex. In contrast, the proximal face is dynamic, and appears to be actively polymerizing and depolymerizing. Bar=5 μm.

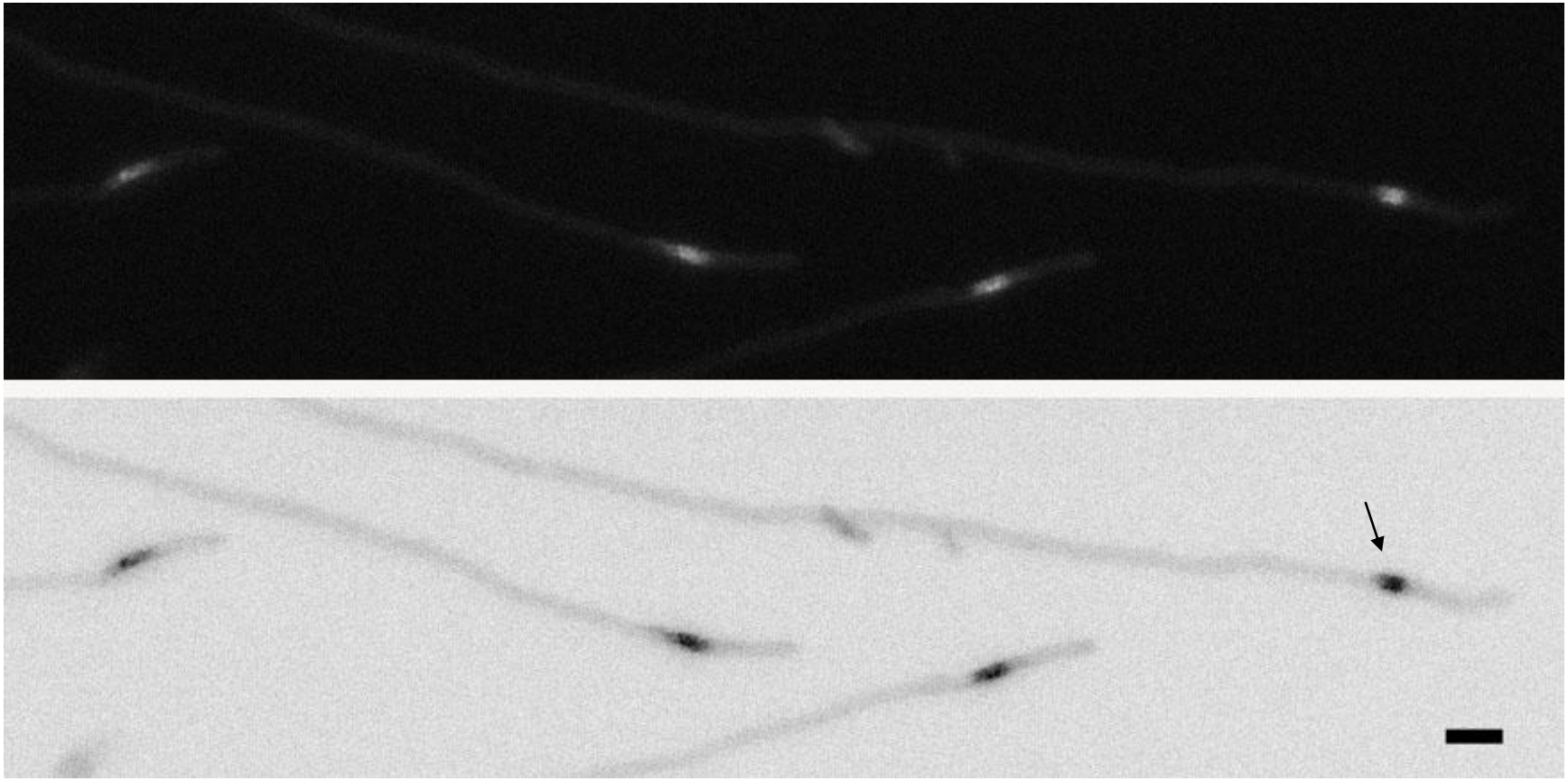

Figure 17. SAW structures are localized in multiple hypha throughout the mycelium. The monochrome and inverted monochrome image show that actin cables organize to form a mesh-like structure, known as the SAW (arrow), which is located in the subapical region of the hyphae. The SAW maintains a relative distance distal from the tip in each of the hyphae, approximately 6.2 μm. The average growth rate of hypha where the SAW is present is 0.7 μm per minute, with a standard deviation of 1.0 μ/min. Bar=10 μm.

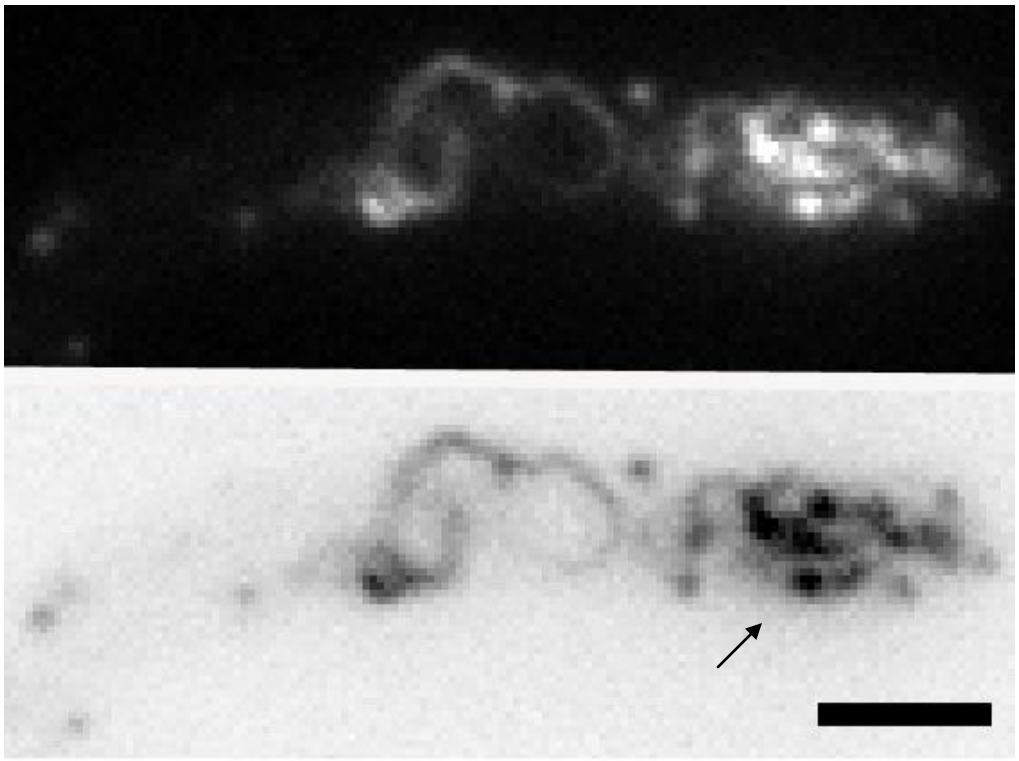

Figure 18. Actin cables localize to form the AAA. The monochrome and inverted monochrome image shows that actin cables organize to form a mesh-like structure, known as the AAA (arrow). The AAA is located in the apical region of the hyphae and exhibits distinct dynamics. The face within the apex is typically stable, whereas the cables at the distal face are dynamic and exhibit retrograde treadmilling. These patterns are antithetical to what has been observed in the SAW. Bar=5 μm.

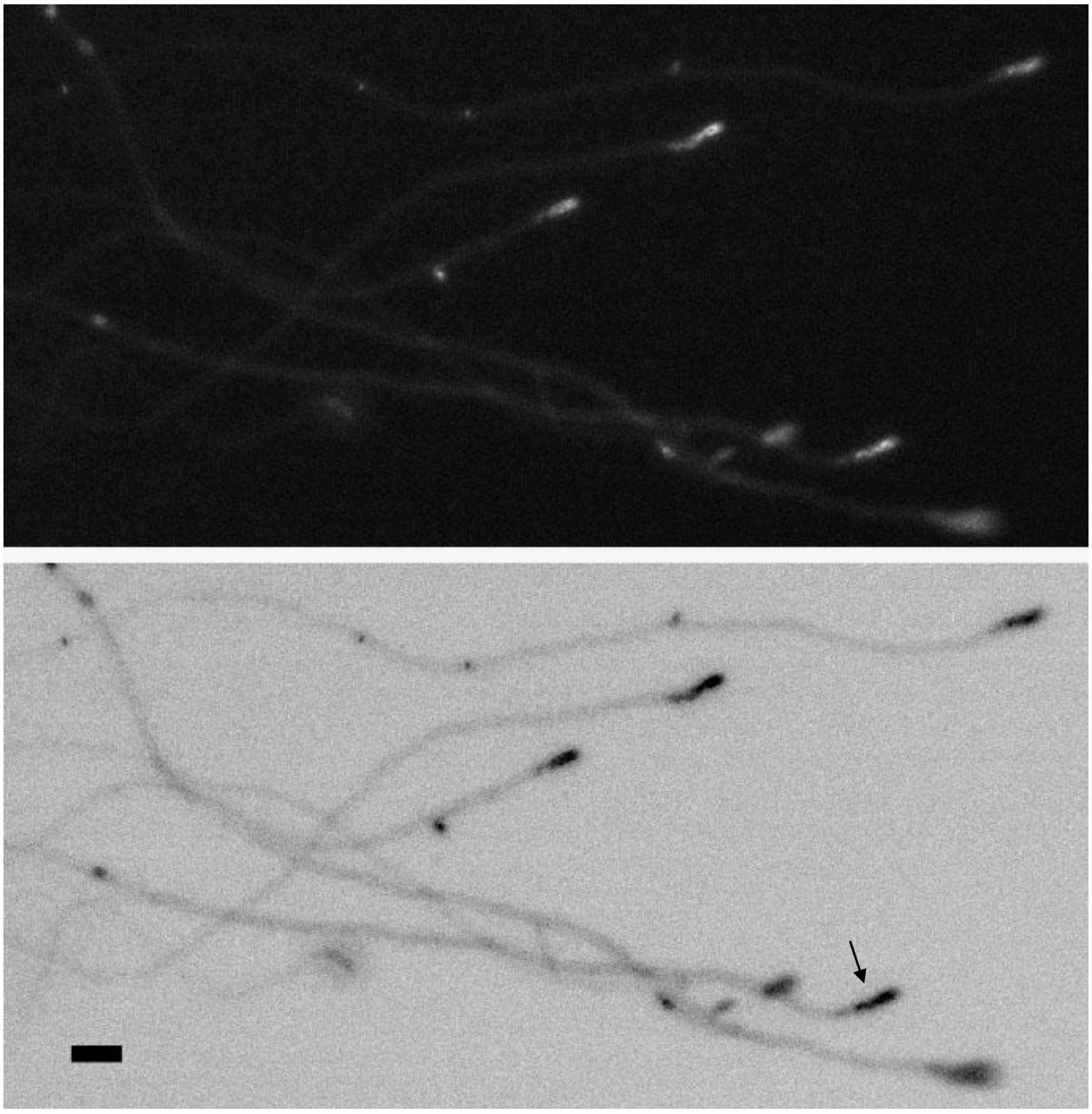

Figure 19. AAA structures are localized in multiple hypha throughout the mycelium. The monochrome and inverted monochrome image shows that actin cables organize to form a mesh-like structure, known as the AAA (arrow), which is located in the apical region of the hyphae. The AAA maintains a relative distance distal from the tip in each of the hyphae. The average growth rate of hypha where the AAA is present is 0.4 μm per minute, with a standard deviation of 0.2 μm/min. Bar=10 μm.

TABLES

Table 1. Strain genotypes and sources

Strains	**Genotype**	**Source**
A773	*pyrG89; wA3; pyroA4; veA1*	FGSC*
LQ1	*pyrG89; wA3; veA1*	This study
LQrss3	*pyrG89::niiA(p)*::lifeact-tagrfp*; pyroA4; wA3; veA1; A.fpyrG*	This study
LQG11	*Ccg-1(p)*::lifeact::sGFP::bar+;*pyrG89; pyroA4; wA3; veA1; AfpyrG*	This study

*Fungal Genetic Stock Center (McCluskey, 2003)

Table 2. Subapical Actin Web (SAW) and Apical Actin Array (AAA) Analysis

	SAW	AAA
Percentage of the total hyphae observed (%)	36.7	63.3
Average distance from the actin structure to the apex (µm)	6.2	
Standard deviation of the average distance (µm)	2.1	
Average rate of hyphal growth (µm/min)	0.7	0.4
Standard deviation of the rate of hyphal growth (µm/min)	1.0	0.2